RESEARCH

2007-51

Employment of the Traffic Management Lab for the Evaluation and Improvement of Stratified Metering Algorithm

Phase IV

Technical Report Documentation Page

1. Report No.	2.	3. Recipients Accession No.
MN/RC 2007-51		

4. Title and Subtitle	5. Report Date
Employment of the Traffic Management Lab for the Evaluation and Improvement of Stratified Metering Algorithm – Phase IV	December 2007 6.

7. Author(s)	8. Performing Organization Report No.
Henry X. Liu, Xinkai Wu, Panos Michalopoulos, John Hourdos	

9. Performing Organization Name and Address	10. Project/Task/Work Unit No.
Department of Civil Engineering University of Minnesota - Twin Cities 500 Pillsbury Drive S.E. Minneapolis, Minnesota 55455	11. Contract (C) or Grant (G) No. (c) 81655 (wo) 252

12. Sponsoring Organization Name and Address	13. Type of Report and Period Covered
Minnesota Department of Transportation 395 John Ireland Boulevard Mail Stop 330 St. Paul, Minnesota 55155	Final Report 14. Sponsoring Agency Code

15. Supplementary Notes
http://www.lrrb.org/PDF/200751.pdf

16. Abstract (Limit: 200 words)

Freeway ramp control has been successfully implemented since mid 60's, as an efficient and viable freeway management strategy. However, the effectiveness of any ramp control strategy is largely dependent on optimum parameter values which are preferably determined prior to deployment. This is certainly the case happening to the current Stratified Zone Metering (SZM) strategy deployed in the 260 miles freeway network of Minneapolis – St. Paul metropolitan area. In order to improve the performance of the SZM, which highly depends on the values of more than 20 parameters, this research first proposed a general methodology for site-specific performance optimization of ramp control strategies using a microscopic simulation environment, as an alternative to trial and error field experimentation, and implemented the methodology to the SZM. The testing results show that the new SZM control with site-specific optimum parameter values significantly improves the performance of freeway system compared with the original SZM strategy. Secondly, this research proposed a methodology to explore the common optimum parameter values for the current SZM strategy for the whole Twin Cities freeway system, in order to replace the site-specific optimum values which have minor practical value because of the difficulties in implementation and numerous time-consumption to search the site-specific optimum values for all the freeway sections. The common parameter values are identified applying the Response Surface Methodology (RSM) based on 4 specifically selected freeway sections which can represent all types of freeway sections in Minneapolis-St. Paul metropolitan area.

17. Document Analysis/Descriptors	18. Availability Statement
Ramp Metering, Stratified Zone Metering, Ramp Queue Estimation	No restrictions. Document available from: National Technical Information Services, Springfield, Virginia 22161

19. Security Class (this report)	20. Security Class (this page)	21. No. of Pages	22. Price
Unclassified	Unclassified	91	

Employment of the Traffic Management Lab for the Evaluation and Improvement of Stratified Metering Algorithm

Phase IV

Final Report

Prepared by:

Henry Liu
Xinkai Wu
Panos Michalopoulos
John Hourdos

Department of Civil Engineering
University of Minnesota

December 2007

Published by:

Minnesota Department of Transportation
Research Services Section
395 John Ireland Boulevard, MS 330
St. Paul, Minnesota 55155-1899

Acknowledgements

The authors wish to express appreciation to Regional Traffic Management Center (RTMC) of the Minnesota Department of Transportation (Mn/DOT) for its continuing trust and support. Specifically the authors are indebted to Mr. James Kranig, Mr. Brian Kary, Mr. Todd Kramascz and Mr. J. Antonio Fischer for their valuable contribution and cooperation. Additionally, the authors would like to thank Adinarayana Beegala for his assistance.

Table of Contents

List of Tables

List of Figures

Executive Summary

Freeway ramp control has been successfully implemented since mid-1960s, as an efficient and viable freeway management strategy. However, the effectiveness of any ramp control strategy is largely dependent on optimum parameter values that are preferably determined prior to deployment. This is certainly the case with the current Stratified Zone Metering (SZM) strategy deployed in the 260 miles of freeway network in the Minneapolis – St. Paul metropolitan area. To improve the performance of the SZM, which highly depends on the values of more than 20 parameters, this research first proposed a general methodology for site-specific performance optimization of ramp control strategies using a microscopic simulation environment, as an alternative to trial-and-error field experimentation, and implemented the methodology to the SZM. The testing results show that the new SZM control with site-specific optimum parameter values significantly improves the performance of the freeway system compared with the original SZM strategy.

Second, this research proposed a methodology to explore the common optimum parameter values for the current SZM strategy for the whole Twin Cities freeway system to replace the site-specific optimum values which have minor practical value because of the difficulties in implementation and the amount of time it takes to search the site-specific optimum values for all the freeway sections. The common parameter values are identified applying the Response Surface Methodology (RSM) based on four selected freeway sections, which represent all types of freeway sections in the Minneapolis-St. Paul metropolitan area. The common optimum parameter values are implemented in SZM to compare with the original strategy as well as the improved control with site-specific optimum parameter values through simulation. The testing results show that the improvement of SZM control with common optimum parameter values is not as good as the control with site-specific optimum parameters, but the difference is very small: Compared with the original SZM strategy, however, performance is significantly improved. Most important, the improved SZM with common parameter values does not violate the ramp waiting time constraint.

Part I Introduction and Background

1. INTRODUCTION

1.1 Problem Statement

Travel demand has been growing at an enormous rate for the past few decades. Since 1970, the U.S. population has increased by 38 percent, licensed drivers have grown by 71 percent, registered vehicles increased by 99 percent and the number of miles driven every year has increased by 148 percent. Yet during that same period, there has been a scant six percent increase in road miles. Consequently, traffic congestion has increased immensely, particularly in urban areas and along heavily-traveled intercity corridors. The annual cost of congestion in the United States due to lost productivity alone, excluding the costs of wasted fuel and environmental impacts, is about $100 billion (ITS America, 1995). Further, traffic safety is also jeopardized due to increasing congestion. According to National ITS Program Plan 1995 by ITS America, each year traffic accidents result in over 41,000 fatalities and 5 million injuries, at an additional cost of $137 billion to the Nation's economy. Highway Statistics (Federal Highway Administration, 2000) show that a large portion of the fatalities, more than 6,940, are freeway related. However, the advent of Intelligent Transportation Systems (ITS) has opened up potential solutions that can collectively go a long way in improving transportation efficiency and safety. In particular, ramp metering as an Advanced Traffic Management System (ATMS) and a vital functional area of ITS, has been one of the most effective control measures in alleviating freeway congestion. The general objective of ramp control is to maintain freeway volume below its operational capacity by controlling access at entrance ramps. In effect, ramp control improves freeway capacity utilization, increases throughput, reduces recurrent and non recurrent congestion and thereby minimizes system delay (Papageorgiou et al., 1997). Ramp meters also enable efficient and safe merging operations by breaking platoons of vehicles released from nearby signalized intersections (Elefteriadou, 1997). According to a study by the Federal Highway Administration (Arnold, 1998), ramp control systems in the US and Canada result in 16-62% increase in average freeway speeds, up to 48% decrease in total travel time and 15-50% decrease in accidents.

Even though the benefits from ramp metering are clear, they can be achieved only when ramp meters are implemented and operated effectively (Pearce, 2000). Specifically, the effectiveness of a ramp control strategy is largely dependent on the values of the parameters. However, in practice, ramp control strategies are customized empirically and calibrated in the field over a period of time through trial and error. Although such an empirical approach can be effective, there is no assurance that it is the best for a particular freeway, as it takes time to fine-tune a control strategy and also often adversely affects traffic flow resulting in driver frustration. Furthermore, such an approach is limited in breadth of search and generally leads to an acceptable rather than best performance as the deviation from optimality is unknown. As advanced coordinated traffic responsive ramp control strategies start to emerge, the need to develop a

systematic and efficient procedure to calibrate complex ramp control algorithms was recognized (Zhang et. al., 2001, Xin et al., 2004). However, research on performance optimization of field deployed ramp control strategies is only recent limiting the available methodologies which are yet impractical for general implementation on area wide coordinated ramp metering algorithms.

1.2 Research Objectives

The objective of this study can be summarized as follows:

- Develop a general methodology for optimizing the performance of ramp control strategies prior to implementation. This required development of a hybrid simulation based optimization framework and enhancement of the microscopic simulator.
- Demonstrate the applicability of the methodology through implementation on a specific control strategy. Twin Cities' current Stratified Zone Metering strategy is selected and the results are assessed at two typical Twin Cities' test sites
- Develop a methodology for expanding the site-specific parameter values to common values for a whole metropolitan area. And applying the proposed methodology, identify the common parameter values for SZM in the whole Twin Cities.
- Evaluate the methodology using microscopic simulation.

1.3 Report Organization

This report is organized into 4 parts. Part I presents a literature review of performance optimization/calibration of ramp control strategies along with a background on most recent operational ramp control strategy, Minnesota's Stratified Zone Metering (SZM). Part II presents a general methodology for the site-specific performance optimization of ramp control strategies with detailed framework of sensitivity analysis and RSM optimization. And this methodology is demonstrated through implementation on one of the most recent coordinated traffic responsive ramp control strategies, the Stratified Zone Metering (SZM).Part III proposes a methodology to explore the common parameter values for a ramp control algorithm and identifies the common parameters value for the SZM strategy for the whole Twin Cities area. Finally, Part IV presents a summary of findings with concluding remarks and future research directions.

2. BACKGROUND

2.1 Literature Review

There is a large body of theoretical research in the literature that deals with the application of optimization techniques to ramp control problems. One of the very first attempts in this direction (Wattleworth, 1967) involved application of linear programming in time independent optimization to maximize freeway throughput subject to freeway capacity constraints. Following this, optimal control theory and time-discrete form of macroscopic flow models were combined to achieve coordinated ramp control (Papageorgiou 1983, Stephanedes and Chang, 1993, Zhang et al. 1996, Chang et al. 2002). In spite of some significant developments in the class of optimal ramp control, due to their computational complexity and the inaccuracies involved in the OD estimation process, their practical implications have been limited.

On the other hand, over the years numerous operational ramp control strategies have been developed and deployed in practice. Some noteworthy examples of field deployed integrated ramp control include ZONE and STRATIFIED Metering in Twin Cities, Minnesota; BOTTLENECK algorithm in Seattle, Washington; HELPER algorithm in Denver, Colorado; SWARM in Orange County, California; METALINE in Paris and Amsterdam. In addition to these, there are a number of proposed ramp metering algorithms awaiting further assessment and future implementation (see Bogenberger and May, 1999). However, research on optimizing or systematically calibrating the performance of such complex algorithms is very limited. Hasan et al. (2002) calibrated two of the four operational parameters of ALINEA and FLOW ramp control strategies by setting definite levels for each parameter, evaluating all possible parameter combinations in different scenarios, and selecting the best parameter combination. Being a very exhaustive search technique, this method was feasible only because two parameters were calibrated on each algorithm. As the size of the parameter set increases, which is generally the case in more complex algorithms, this method becomes extremely computationally intensive and thus impractical. In another recent study Chu and Yang, (2003) presented a hybrid Genetic Algorithm-Simulation method to optimize the operational parameters of ALINEA ramp control, as an alternative to real world trial and error testing. Even though the method was effective in this case, it is worthwhile noting that ALINEA is a local ramp control with only four control parameters to optimize. Park and Carter (1995) pointed out that as problem size (number of parameters) increases, the performance of a genetic search degrades drastically as numerous evaluations will be required for convergence. With only four parameters, optimization of ALINEA required 100 evaluations (~30 days of CPU Time). Further, Genetic Algorithms are incapable of estimating relative importance of parameters and their mutual interactions. GA also assumes that the parameters are independent to each other and a value assumed by one parameter will not affect the instantiation of other parameters. It has been suggested that high Epistatis (Interaction between parameters) is the reason for the failure of GA in certain problems (Goldberg, 1989).

2.2 Stratified Zone Metering

The Minnesota Department of Transportation (Mn/DOT) operates nearly 430 ramp meters to control access on approximately 210 miles of freeway in the Twin Cities Metropolitan area. An integrated system wide traffic responsive ramp control strategy, ZONE metering had been successful for the last few decades in alleviating congestion on the Twin cities' freeways. However, excessive ramp delays due to freeway demand surge on specific ramps mandated an 8-week ramp meter shutdown study (Cambridge Systematics, 2001). The study confirmed the overall system wide benefits of ramp metering. Nevertheless, the findings also showed that, as the objective of Zone metering strategy focuses only on maximizing freeway throughput, ramp queues remain unchecked thereby resulting in unacceptable ramp delays and spillbacks.

Following the shutdown study, MnDOT modified the control objective to implement a queue control policy and devised the new Stratified Zone Metering algorithm (henceforward referred to as SZM). The objective of the new strategy is still the same as to maximize freeway throughput but with an additional constraint to limit the waiting time on the ramps to a predetermined maximum. The implementation of SZM in the Twin Cities metro area started in March 2002 and it has been only recently that its full deployment was accomplished.

To help identify all the parameters and their importance in the Stratified ramp control, a concise description of the algorithm is presented here. Interested readers can find a detailed description along with an illustrative example of design of the algorithm in Xin et al., 2004 and Lau, 2001. In this report all the parameters of the SZM control strategy represented in bold typeface.

2.2.1. Data Processing

The functionality of SZM control strategy is entirely dependent on real time 30 second occupancy and volume data from the loop detectors in the metro area. Unlike occupancy, volume counts are discrete and when converted to hourly rates these discontinuities blow up resulting in a flow rate function with noise. Hence, all hourly flow rates need to be smoothed by a floating average to capture overall trends. Smoothing in SZM algorithm is done according to the following equation

$$F_t = F_{t-1} + K * (G_t - F_{t-1}) \qquad (2\text{-}1)$$

where, t = 1,2,3…is the sampling index;

F_t and F_{t-1} are the smoothed flow rates for the current and previous sampling intervals respectively;

G_t is the current unsmoothed hourly flow rate; and

K is a smoothing constant that indicates degree of smoothing.

2.2.1.1. Ramp Demand Processing

Ramp demand processing is the first step in the control logic. On each ramp, typically two types of detectors are deployed to measure the ramp demand in real time; a queue detector at the upstream end of the ramp and a passage detector immediately downstream to the ramp meter.

Ramp demand is the smoothed hourly flow rate calculated from the 30 second volume counts typically from a queue detector. In case of malfunctioning or absence of a queue detector, passage detector volume counts are used. However, as a passage detector cannot measure the true entrance demand, its 30 second volume is increased by a factor to prevent excessive queuing. This factor is called the Passage Correction factor ***(P_c)***.

$$D_t = D_{t-1} + K_P * (P_c * V_t - F_{t-1}) \quad (2\text{-}2)$$

where

K_P is the ramp demand smoothing factor

When the ramp queue extends beyond its queue detector, the queue detector no longer gives an accurate measurement of the ramp demand. Such a condition is identified from the high occupancy measurements at the queue detector. Hence, whenever queue detector occupancy exceeds an empirically determined threshold ***($O_{threshold}$**: 25%)*, a 30-second step increment in ramp demand ***(I_{ramp}**: 150 veh/hr)* is added to the smoothed flow rate.

2.2.1.2. Ramp Queue Control

Estimation of ramp queue is of prime importance to the SZM control strategy as the strategy aims to restrict the maximum waiting time on a ramp. The queue size is calculated as the product of queue storage length *(L)* and queue density *(Q_d)*.

$$N = Q_d * L \quad (2\text{-}3)$$

where

L is the queue storage length in feet between the ramp meter and the queue detector

Q_d is the queue density estimated using a smoothed metering release rate called the accumulated release rate (R_a).

$$Q_d = 206.715 - 0.03445 * R_a \quad (2\text{-}4)$$

The queue density estimation based on the above equation is empirical but proved statistically significant throughout the control period. However, efforts for further improvement in the accuracy of the queue estimation are underway. In scope of the present study, the sensitivity of this equation is indirectly tested by considering the slope *(Q_{slope}: -0.03445)* and intercept *($Q_{Intercept}$: 206.715)* of the queue estimation equation as parameters of the algorithm.

To keep the ramp wait times below a predetermined Maximum Waiting Time Threshold (T_{max}), for each metered ramp a Minimum Release Rate *(r_{min})* is calculated based on the estimated queue size. Thus, to ensure that the last vehicle in the queue will not wait more than T_{max}, the ramp's minimum release rate for that control interval should be,

$$r_{\min} = \frac{N}{T_{\max}} \tag{2-5}$$

where N is the queue size estimated from Eq.(3)

Minimum release rate determined as above should be in between an Absolute maximum Release rate *(R_{max} : 1714 veh/hr)* and Absolute Minimum Release rate *(R_{min} : 240 veh/hr).* Metering rate is adjusted accordingly if not within this range.

2.2.2. Zone Flow Balance

Zone Flow Balance is the central element of Stratified Zone Metering control. A Zone is defined as a continuous stretch of freeway with mainline detector stations as end points. It is identified as a group of consecutive mainline stations with number of stations in a zone varying from two to seven. Thus, the entire freeway segment is divided into groups of zones containing 2, 3…7 consecutive stations. Each such Zone group constitutes a Layer. As there are zones of six different sizes, six layers can be identified one for each zone size (refer figure 2.1). In other words, all mainline stations on the entire freeway are grouped in sets of two, three, and so on up to seven, and all consecutive zones with same number of stations are said to form a layer. Therefore, every mainline station (with an exception for those near the boundaries) gets associated with six zones upstream and six zones downstream to it. As it can be readily seen, Zones overlap with zones of other sizes (refer figure 2.3). The concept behind choosing the maximum number of stations in a zone to be seven is that it is believed that to alleviate a bottleneck, controlling meters within a distance of 3 miles (stations are approximately half a mile apart) is sufficient for the next control interval of 30 seconds.

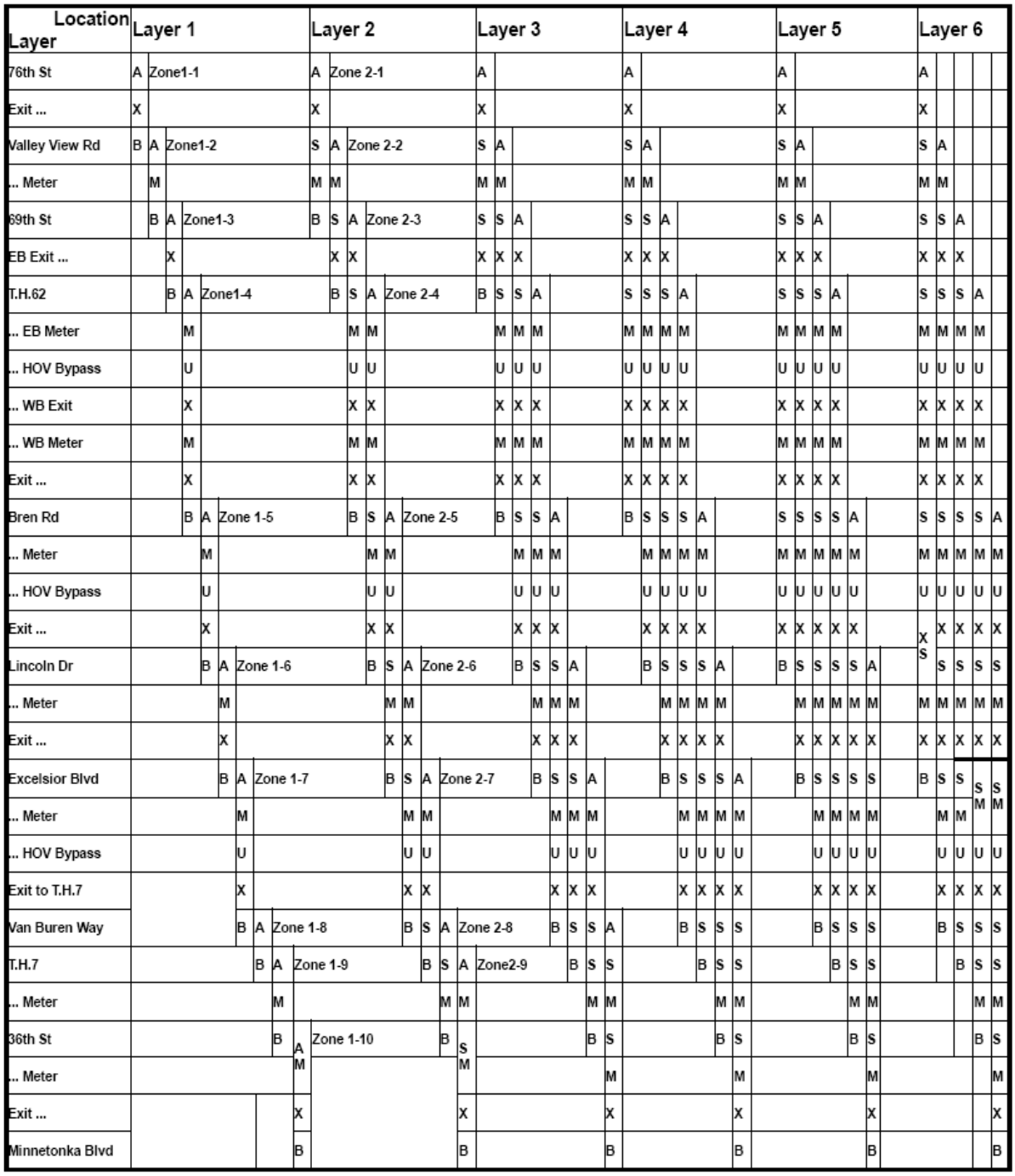

A - Upstream station, X - Exit ramp, B - Downstream station, M - Metered ramp, U - Unmetered ramp

Figure 2- 1 Stratified Zone Metering Example (TH 169 NB)

A layer is defined as a continuous stretch of all successive zones of the same size. As there are zones of six different sizes, six layers can be identified one for each zone size (refer fig 2.3). As it can be readily seen, zones overlap extensively, within and across layers. This Zone-Layer structure enables SZM to achieve a system wide control. Moreover, unlike its predecessor, identification of potential bottlenecks is not required in the SZM control due to an extensive overlap of zones.

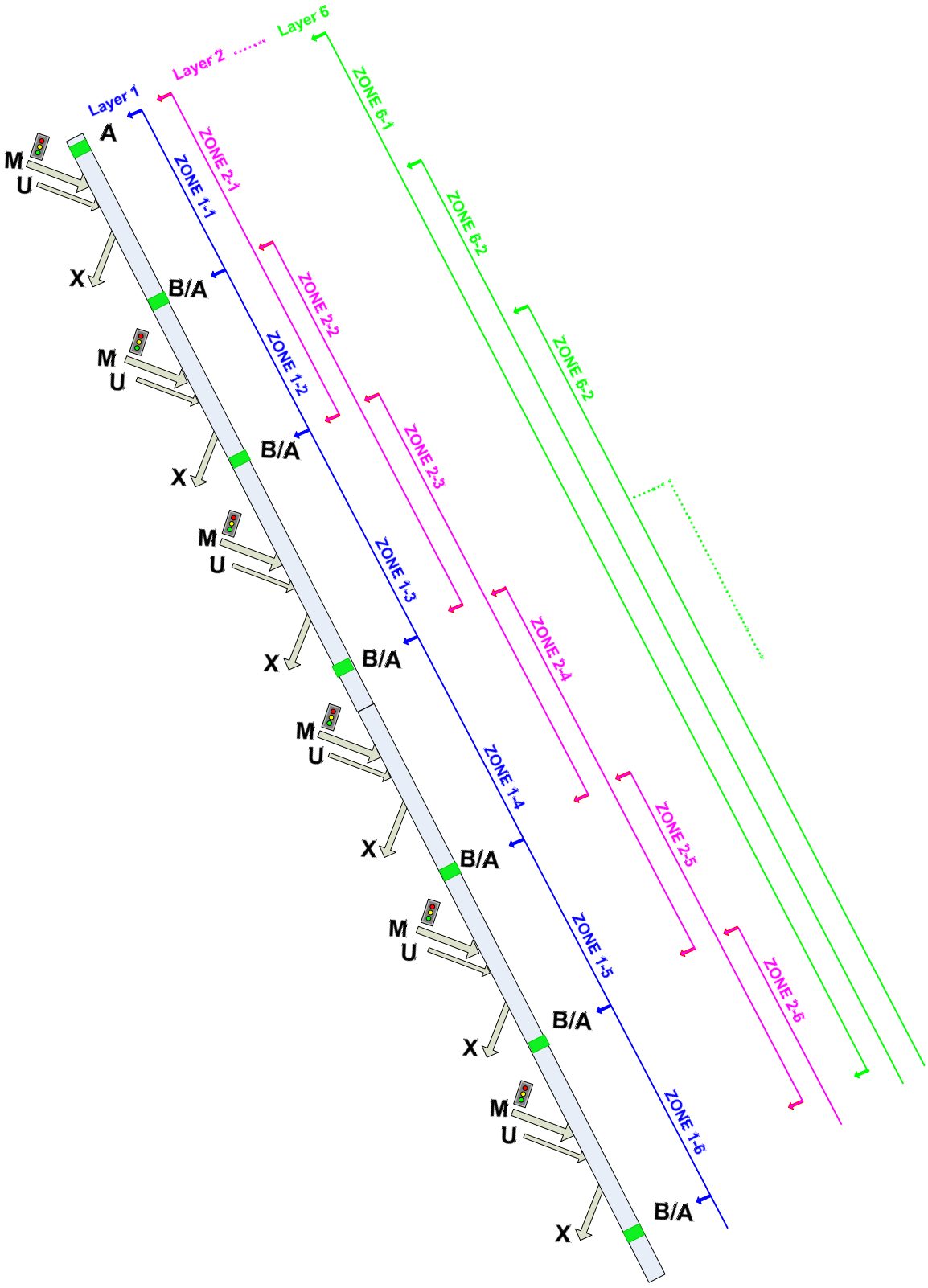

Figure 2- 2 Zone-Layer Structure of Stratified Zone Metering

Once the zone-layer structure is built, the next step is to process what is known as a metering rule. A metering rule is a zone inequality which reflects the basic control objective of SZM; to maintain the number of vehicles entering a zone less than that leaving the zone. In terms of the possible inputs and output flows within a given zone, the zone inequality takes the form as:

$$M + A + U \leq B + X + S$$

i.e.,

$$M \leq B + X + S - A - U \qquad (2\text{-}6)$$

where,

M is the total metered entrance ramp flow (controlled by the Algorithm)

A is the measured upstream mainline flow

U is the total measured unmetered entrance ramp flow

X is the total measured exit ramp flow

B is the downstream mainline capacity

S is the spare capacity on the mainline

Upstream mainline flow A, unmetered entrance ramp U and exit ramp flow X are smoothed based on Eq. (1) using their corresponding smoothing constants $\boldsymbol{K_M}$, $\boldsymbol{K_U}$ and $\boldsymbol{K_X}$ respectively. Just as the ramp demand smoothing constant $\boldsymbol{K_D}$, the constants $\boldsymbol{K_M}$, $\boldsymbol{K_U}$ and $\boldsymbol{K_X}$ smoothing constants are also the parameters of the algorithm and are included in the present study.

The downstream mainline capacity *(B)* is the expected mainline capacity at that location. It is calculated based on the capacity estimate of rightmost lane *(**C_R**)* and the capacity estimate for other lanes *(**C_O**)*. Specifically,

$$DownstreamMainlineCapacity(B) = C_R + (NumberOfLanes - 1) * C_O \qquad (2\text{-}7)$$

where, capacity estimates $\boldsymbol{C_R}$ and $\boldsymbol{C_O}$ are the parameters of the algorithm

The term Spare capacity *(S)* is introduced to measure the unoccupied capacity in the zone so that the ramp meters that are affected by the zone's rule, can be less restrictive than otherwise. More specifically, spare capacity is calculated as,

$$S = (FullDensity - ZoneDensty) * LaneMiles \quad (2\text{-}8)$$

where*, FullDensity (*$\mathbf{D_f}$*: 32 veh/mile)*, a parameter of the algorithm, is a predefined threshold of density, above which the mainline is regarded to have no spare capacity left. It should be noted that this threshold is not meant to be an indicator of the onset of congestion.

The process of distributing a zone's maximum allowed metered input *(M)* among its metered ramps is known as zone's rule processing. Under Stratified Zone Metering, zones are processed sequentially based on layers; starting from the first zone in the first layer to the last zone in the sixth layer. For each zone in this sequence, the rule processing is done as follows:

i) Calculate the total allowed metered entrance ramp input *(M)* into the zone using Eq. (6)

ii) Calculate the sum of the demands from all the metered ramps within the zone

$$\sum_i D = D_1 + D_2 + D_3 + ... + D_n \quad (2\text{-}9)$$

where *n* is the number of metered ramps within the zone

iii) Propose a weighted release rate *(* R_i^p *)* for each metered ramp, in proportion to the individual ramp demand *(*D_i*)*

$$R_i^p = M * \left[\frac{D_i}{\sum_i D_i} \right] \quad \forall \ i = 1, 2, 3 \ldots n \quad (2\text{-}10)$$

iv) All metered ramps in the zone, at this moment, should have *minimum release rate (*r_{min} *from Eq.5),* a *release rate* proposed from a previous rule processing and the new *proposed release rate (* R_i^p from *Eq.10).* The initial value of the *release rate* is set to the *Maximum release rate (*$\mathbf{R_{max}}$*: 1714 veh/hr)* and may get modified as the zones are processed. The *proposed release rate* R_i^p is compared with the *minimum release rate* and *release rate* for each ramp meter and such a comparison results in zone balance. If the *proposed rate* is less than the *minimum release rate*, the zone balance is reduced by the difference while if the *proposed rate* is greater than the *release rate*, the zone balance is increased by the difference

v) If the zone balance is below zero, each meter that reduced the zone balance gets it finalized release rate as the minimum release rate. Otherwise, the release rates of all the meters that increased the balance remain unchanged. Then the zone is processed again excluding the finalized meters and deducting their respective release rates from the total allowed metered input *(M)*. This iterative process continues until a zero zone balance is achieved.

This rule processing is done sequentially for all zones in all layers and this finalizes the release rates of all metered ramps as *field rates* for the next 30-second control interval.

All the control parameters of the SZM control are tabulated along with their current practice default values in Table 2.1.

Table 2- 1 Control Parameters of Stratified Zone Metering

No:	SZM Control Parameter	Notation	Units	Current Value
1	Absolute Maximum Release Rate	R_{max}	Veh/hr	1714
2	Absolute Minimum Release Rate	R_{min}	Veh/hr	240
3	Increment to ramp demand	I_{ramp}	Veh/hr	150
4	Full Density of a zone	D_f	Veh/mile	32
5	Max. Allowed waiting time on Local ramps	$T_{max,\,L}$	Seconds	240
6	Max. Allowed waiting time on F-F ramps	$T_{max,F}$	Seconds	120
7	Queue Density equation-Intercept	$Q_{Intrecept}$	Veh/mile	206.715
8	Queue Density equation-Slope	Q_{Slope}	Hr/mile	0.03445
9	Capacity Estimate for Rightmost mainline lane	C_R	Veh/hr	1800
10	Capacity Estimate for Other mainline lanes	C_O	Veh/hr	2100
11	Occupancy Threshold	O_{Th}	%	25
12	Ramp Meter Turn off threshold	M_{off}	%	80
13	Ramp Meter Turn on threshold	M_{on}	%	85
14	Passage Compensate Factor	P_c	-	1.15
15	Accumulate Release rate smoothing factor	K_R	-	0.20
16	Queue Detector smoothing factor	K_D	-	0.15
17	Passage Detector smoothing factor	K_P	-	0.20
18	Mainline station smoothing factor	K_M	-	0.15
19	Unmetered station smoothing factor	K_U	-	0.15
20	Exit station smoothing factor	K_X	-	0.15

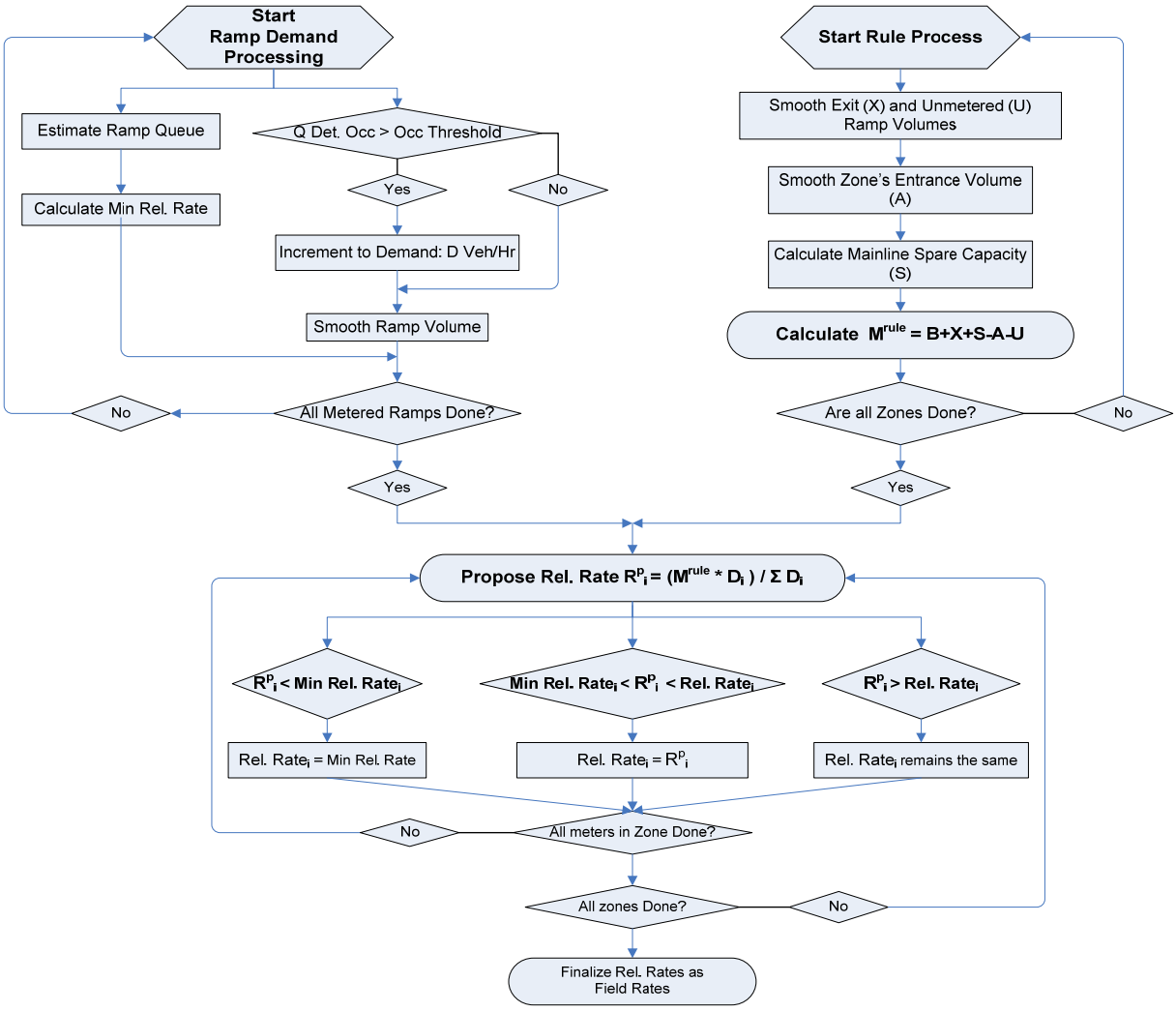

Figure 2- 3 Structure of Stratified Zone Metering Algorithm

Part II Site-Specific Parameter Optimization

3. PERFORMANCE EVALUATION FRAMEWORK

The proposed methodology to optimize the performance of on-ramp control strategies comprises of two steps. The first step is to identify the parameters of the ramp control algorithm that most strongly influence its performance. This is a stage of detailed sensitivity analysis of the control parameters with a preliminary screening followed by a robust analysis to identify significant main effects and interactions among the parameters. The second step is to obtain optimal values for the parameters identified as significant in the first step. This is achieved by applying general principles of Response Surface Methodology (Box and Wilson, 1951) for the optimization of black box models. Prior to implementing the methodology it is required to first define performance measure(s) that will be used as optimization objective function(s) and further also develop an evaluation framework for the estimation.

3.1 Performance MOEs

Performance of ramp control strategies can be evaluated from a number of perspectives; typically considered by traffic engineers are:

Efficiency and Equity:	Total System Delay	Total Mainline Delay
	Total Ramp delay	Average Mainline Speed
	Total Travel	Freeway Throughput
	Travel Time Reliability	
Transportation Safety:	Accident rate	
	Total Number of Stops	
Environmental Impact:	Pollutant Emissions	
	Fuel Consumption	

Depending on the evaluation objective, generally one or more of the above alternatives is selected. In this study, as drivers are most sensitive to delays, total travel delay was originally considered as the Measure of Effectiveness (MOE). However, due to the lack of a consistent definition of delay in the literature, System Total Travel Time, a surrogate

measure of total delay, was finally selected as the primary performance MOE. Further, for a given demand, minimizing System Total Travel Time during the control period is equivalent to minimizing system delay as well as maximizing system throughput. By definition, System Total Travel Time (STTT) includes both Mainline Total Travel Time (MTTT) and Ramp Travel Time (RTTT). As mainline and ramps are two competing sub-systems of the freeway, minimizing System TTT does not simultaneously minimize Mainline TTT and Ramp TTT. Therefore, in addition to STTT, both MTTT and RTTT were also used as optimization objectives for the selected ramp control. In is worth pointing out that a comprehensive optimization should include the entire corridor but this is rarely possible in practice due to the lack of data especially related to volumes on adjacent arterials as well as OD data. Further, OD estimation methods have not yet been used by the practitioners due to the additional time and effort required in the estimation as well as adapting acceptable assumptions. Nevertheless, the methodology presented here is general and could also be adapted to corridors.

In order to estimate the selected performance MOEs, either field operational tests or computer simulation experiments should be conducted. As mentioned in earlier sections, field tests are very expensive, time consuming and risk prone. Besides, the test results are less reliable and inaccurate due to confounding effects of uncontrollable factors like weather conditions, incidents and traffic diversion. For such reasons, simulation has emerged as an excellent tool to study and evaluate the performance of traffic control schemes under controlled conditions. However, as macroscopic and mesoscopic simulators are based on traffic flow models with theoretical limitations, they fail to accurately emulate interrupted flow dynamics such as complex on-ramp merging behavior and weaving which are critical to any ramp control strategy. Microscopic simulators avoid such issues by calculating individual vehicle states in discrete time slices based on vehicle-to-vehicle interactions and thus are deemed more appropriate (albeit not perfect) for performance evaluation of ramp control strategies. In this study, to demonstrate the applicability of the optimization methodology on the Stratified Zone Metering control one of the best microscopic simulators AIMSUN (Advanced Interactive Microscopic Simulator for Urban and Non-Urban Networks) was selected.

3.2 Microscopic Simulator and its Enhancements

3.2.1. Simulator Overview

AIMSUN is an integral part of GETRAM (Barceló et al., 1994), a simulation environment which consists of a traffic network graphical editor called TEDI, a network database, a module for reading from the network database (Pre-simulator), a module for performing the simulation (Simulator), a module for storing results and a Library of sophisticated API (Application Programming Interface) to emulate any user defined control strategy and other ATMS applications. A detailed description of GETRAM Simulation Environment is beyond the scope of this thesis but can be found in Generic Environment for Traffic Analysis and Modeling, Grau, R., Barcelo, J. and Ferrer, J.L.,

1994. Figure 3.1 presents an overall functional structure of AIMSUN and its integration with GETRAM Environment.

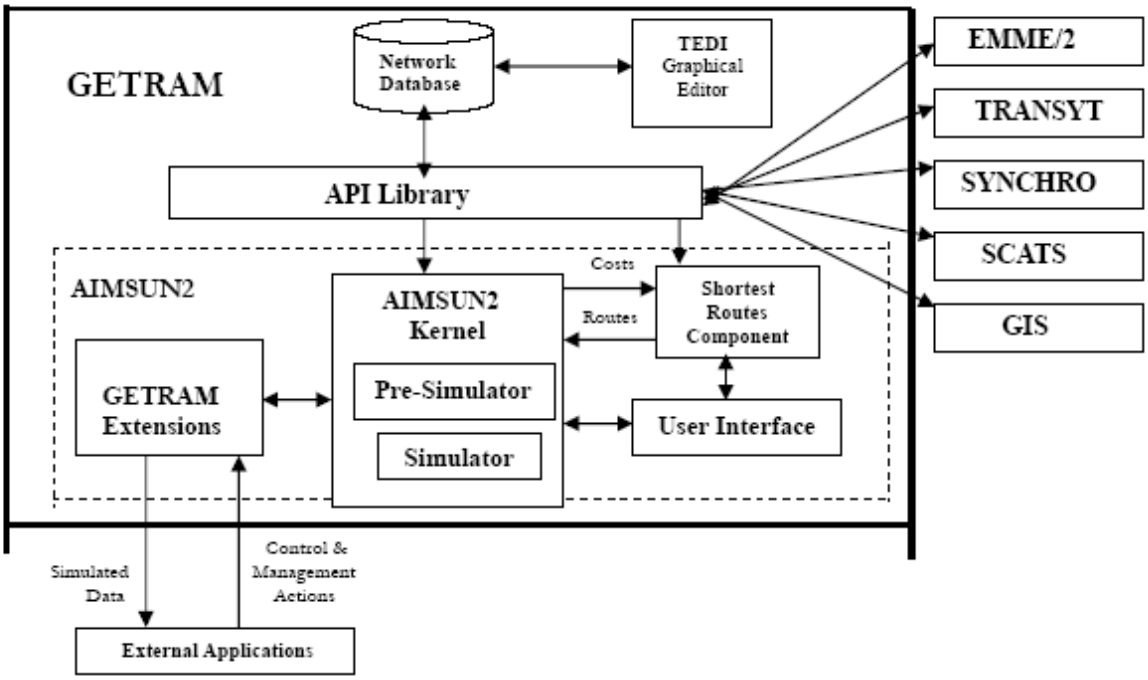

Figure 3- 1 Conceptual Structure of AIMSUN

In AIMSUN, simulation time is split into small time intervals called simulation steps and the vehicles are updated according to vehicle behavior models, car following model and Lane changing model. The car following model implemented in AIMSUN is an ad hoc development of the Gipps model (Gipps, 1986). It was calibrated based on field tests and was further tested on its ability to reproduce macroscopic relationships between fundamental variables. The lane changing behavior in AIMSUM is modeled as a decision process analyzing the necessity of a lane change (to make turnings), the desirability of a lane change (to reach desired speeds) and the feasibility for a lane change (to accept a gap). The actual event of a lane change is governed by a Look Ahead model which captures different lane changing motivations observed among the drives. Two zone distances, corresponding to the discretionary and the forced lane changing behaviors, are identified for the sections that end in a turning movement. Vehicles in the first zone distance tend to get closer to a desired lane and attempt to change lanes without affecting the vehicles in the adjacent lanes. Vehicles within the second zone distance force to reach their desired lanes reducing their speeds and thereby affecting the vehicle behavior in adjacent lanes.

Like most microscopic simulators, AIMSUN also generates outputs which are stochastically distributed. In other words, a simulation model does not provide a unique solution to a given problem as it emulate the behavior of a complex system in which randomness is inherent. The random seed is the only parameter related to randomization. This parameter is an integer used as an initial seed in the pseudo-random number generator of sample real numbers uniformly distributed between 0 and 1. These numbers are used to produce different random distributions which are used to define vehicle arrivals, vehicle characteristics, etc. Thus, using the same random seed always generates identical simulation results. Therefore, a simulation study requires multiple simulation runs using different seed numbers so that the median simulation run or the average results of several simulation runs can reflect average traffic condition of a specific scenario. To determine the number of simulation runs, the mean and variance performance MOEs from simulation results need to be calculated.

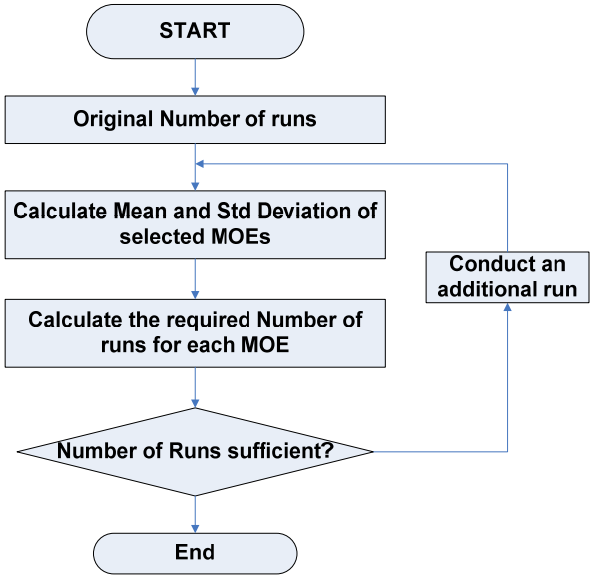

Figure 3- 2 Flow chart for the calculation of number of replications

The number of replications *(N)* required in order to obtain a value within k% of the mean with a α% level of confidence is .

$$N = (t_{\alpha/2}\frac{\delta}{\mu\varepsilon})^2$$

Where μ and δ are the mean and standard deviation of the performance measure based on the already conducted simulation runs; ε is the allowable error specified as a fraction of

the mean μ; $t_{\alpha/2}$ is the critical value of the t-distribution at the confidence level of 1- α. A 97.5% confidence level and a 2.5% allowable error were used in the calculation. In this study, for each of the three selected performance MOEs the required number of replications are calculated and the maximum of all is selected for the entire experiment. Figure 4.2 presents the steps in the form of a flow chart. It has been determined through this procedure that 10 replications are just more than recommended to attain a confidence level of 97.5%. Thus, the average value of all replications was used as the response for each performance MOE. However, for calibration purposes the random seed that generated the median VHT was selected as the representative condition for calibration.

3.2.2. Simulator Enhancements:

AIMSUN provides six high level API functions are defined in order to enable the communication between the AIMSUN simulation model and a user built Getram Extension Module: GetExtLoad, GetExtInit, GetExtManage, GetExtPostManage, GetExtFinish and GetExtUnLoad.

(1) *GetExtLoad():* It is called when the external application is loaded by AIMSUN
(2) *GetExtInit():* It is called when AIMSUN starts the simulation and can be used to initialize the external application
(3) *GetExtManage* (***float*** *time,* ***float*** *timeSta, float timeTrans,* ***float*** *acicle*): This is called every simulation step at the beginning of the cycle, and can be used to request detector measures, vehicle information and interact with junctions, metering and VMS in order to implement the control logic.
(4) *GetExtPostManage (****float*** *time,* ***float*** *timeSta, float timeTrans,* ***float*** *acicle):* This is called in every simulation step at the end of the cycle.
(5) *GetExtFinish():* It is called when AIMSUN finish the simulation and can be used to clear whatever data structures declared in the external applications
(6) *GetExtUnLoad():* It is called when the external application is unloaded by AIMSUN.

Figure 3.3 graphically depicts the interaction between a GETRAM extension module and AIMSUN simulation model.

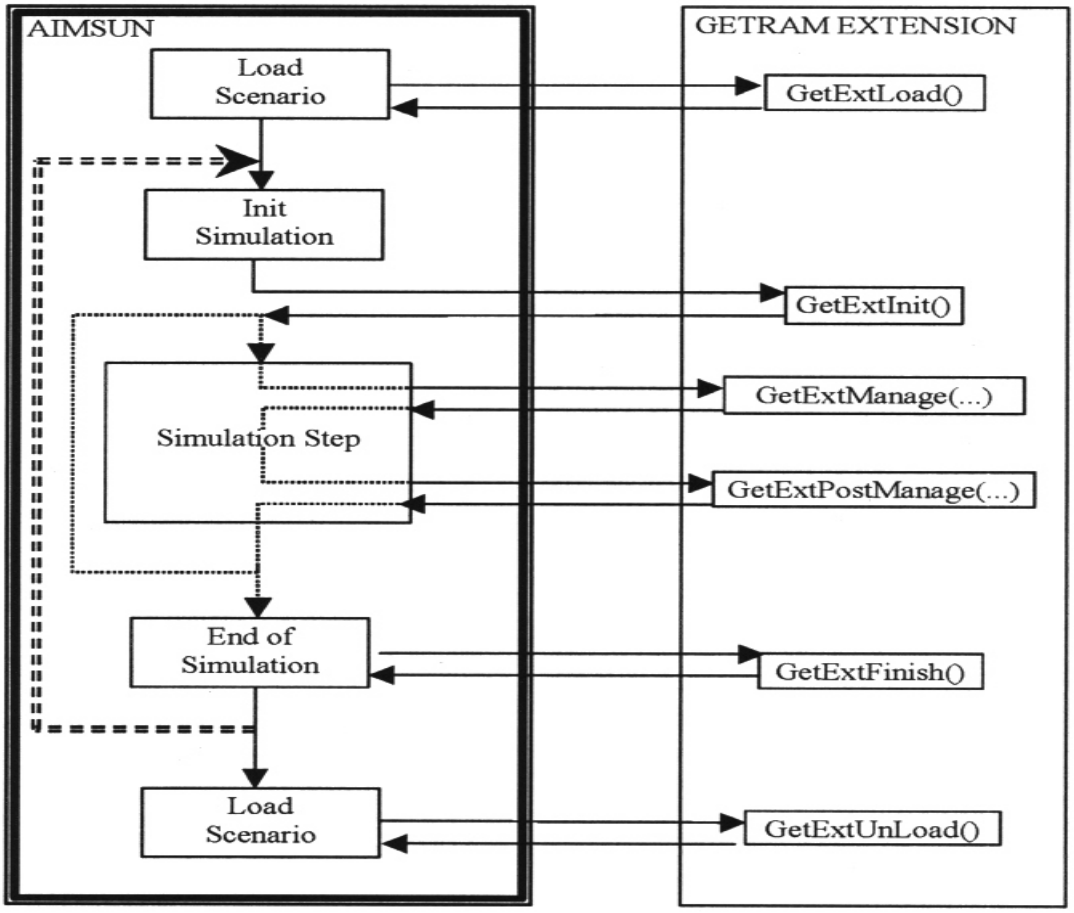

Figure 3- 3 Interaction between GETRAM Extension Module and AIMSUN

The two major enhancements required are:

3.2.1.1. Design of the Control Plan Interface

The design of the CPI is better understood by knowing how the traffic control systems operate in real life. The general process involved in the operation of advanced traffic control systems is as follows: the road network is equipped with traffic detectors with specific layout corresponding to the requirements of the control strategy. The detectors supply the necessary real-time traffic data to the control logic, which after suitable processing makes ad-hoc control decisions such as extending the green phase, changing to the red phase, or applying some traffic calming strategies. These decisions are then relayed to the traffic control devices such as traffic lights, VMS or ramp meters for implementation. In order to simulate this process properly, a simulator needs to be capable of modeling the corresponding traffic devices and emulate their functions in a flexible way, and so requires the Control Plan Interface to be capable of:

- Providing the specific runtime traffic measurements to the control logic at the user defined aggregation time intervals and
- Transferring the ad-hoc control decision from the control logic to the simulation model for implementation.

Essentially the CPI can be considered as a higher-level abstraction that encapsulates the appropriate raw API functions, facilitating the interfacing of AIMSUN with external user-defined ramp control logic. In this way, the CPI ensures the isolation of any ramp control logic from specific roadway geometric layout, allowing one ramp control strategy to be easily replaced with another. As a result, the CPI not only helps test different ramp control strategies on the same network within a single simulator, but also facilitates the finding of optimal operational parameters for a specific control plan, which is the primary objective of this study. Figure 3.4 illustrates the relationship between the simulator, CPI and ramp control logic.

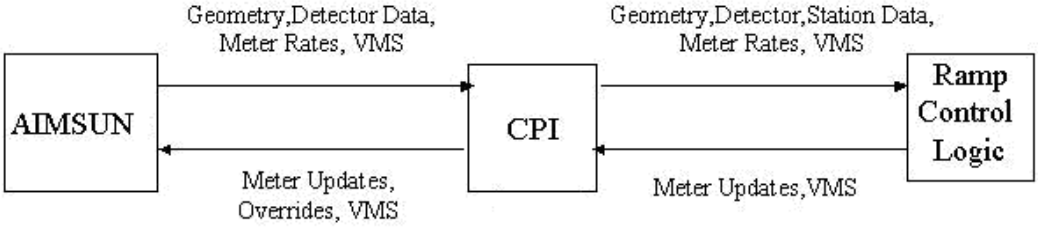

Figure 3- 4 Interactions between AIMSUN, CPI, and Ramp Control Logic

3.2.1.2. Flow of Control in the CPI

The flow of control within the simulator, CPI, and ramp control logic is shown in Figure 3.5. The circles numbered from 1 to 16 represent the steps of the control flowing between the corresponding components. For simplicity, the prefix "circle" is omitted while describing the process.

The first function invoked is GetExtInit. In this function, the input data such as the updating interval for traffic data and ramp control are parsed from an input text file. Appropriate data structure such as the detector maps, station maps and meter maps are declared and initialized in this step (step 1). Next, in the function USER_INITIALIZE the data structures required by the ramp control logic are created and initialized. The default ramp metering rates are returned at this stage (through the step 3 and step 4).

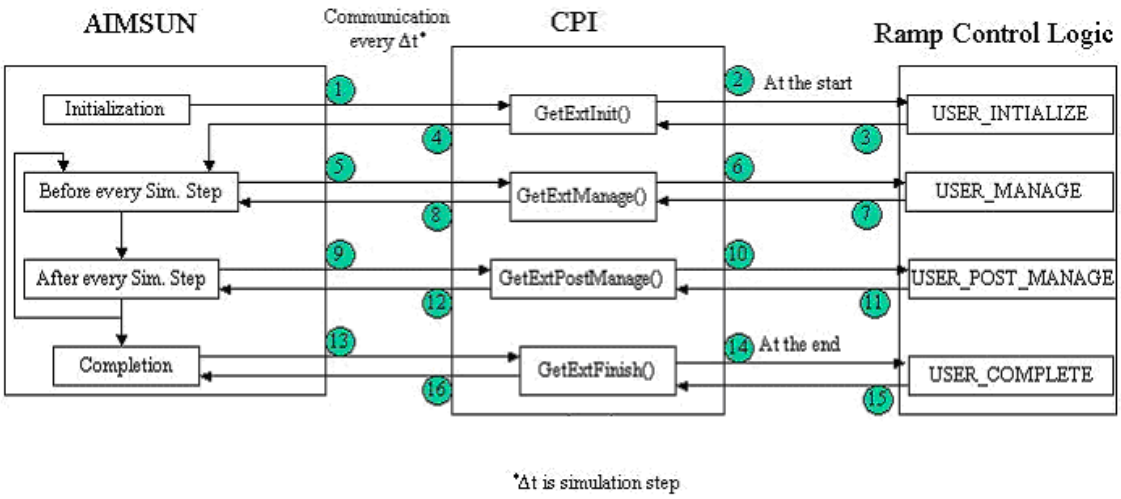

Figure 3- 5 CPI interaction with the Simulator and the Ramp Control Logic

Once the initialization is done, the control is transferred to the function GetExtManage (step 5). In this function the CPI data structures are updated with the runtime simulation data; then the flow of control is passed on to the ramp control logic implemented in the USER_MANAGE function (step 6). The ramp control logic makes decisions for the applicable metering rates to be implemented and returns the ad-hoc decision to the CPI (step 7). Finally, the CPI relays this decision to the simulator for implementation (step 8). After step 8, the control is passed on to the function GetExtPostManage (step 9). This function allows completing whatever tasks necessary. Then the control is transferred to the function USER_POST_MANGE (step 10). Towards the end of the simulation, the function GetExtFinish is called to clear up the data structures defined within the CPI (step 13) while the data structure created for the user-defined ramp control logic is cleared up in the function USER_COMPLETE (step 14).

The Control Plan Interface is developed under the IDE of VC 6.0, using Microsoft Foundation Classes (MFC 4.21). It is in the form of Dynamic Link Library (DLL) that the user can easily integrate to the simulator.

3.3 Emulation of SZM Ramp Control

Having developed the CPI, the further step is to emulate the Mn/DOT's New Statified Zone Metering ramp control, on which the applicability of the optimization methodology will be demonstrated in subsequent chapters. The algorithm is implemented in the simulator by developing the necessary code on top of the CPI. The Visual C++ program has been extensively tested to ensure that the algorithm produced not only the correct final ramp metering rates but also correct output at each and every interim stage of the rates calculation. In order to accurately replicate the control logic, the following two main configuration files are necessary:

Rulefile.txt

In the stratified zone-metering algorithm each segment of the freeway, from a half-mile to three miles in length, constitutes a zone. As these zones within the freeway overlap, the concept of layers has been used in rule processing. The configuration file rulefile.txt provides a sequence of all the detector stations in the same order, as it actually exists on the freeway segment under study. This enables easy identification of all the zones and layers. The file primarily provides the IDs of metered ramps, unmetered stations and exit stations in between two successive mainline stations of the freeway.

The following syntax needs to be maintained in this configuration file:

- The basic format of each line is:

  String_indentifier TAB string TAB string TAB….

- The string identifiers have to be exactly as shown in the table with the order of the lines also being important;
- Each string identifier ends with a colon (:);
- The spacing between the colon and the identifier name can be arbitrary; but it is so chosen that, an indentation is preserved;
- A double asterisk character (‘ ** ’) designates a mainline station entry;
- In case of multiple entries to an identifier, a spacing of one tab between entries is maintained;
- In case of no entry to an identifier, a blank line remains;
- In the last line of rulefile.txt, ‘###END_OF_RULEFILE###’ is used to mark the end of file.

A sample rulefile.txt below shows the syntax to be followed:

Sample configuration file rulefile.txt
**MAINLINE STATION : 428 Metered Ramps : Unmetred station : Exit station : 1039 **MAINLINE STATION : 429 Metered Ramps : 3A2 3A3 Unmetred station : 1349 Exit station : 1117 1365 **MAINLINE STATION : 430 … … … … ###END_OF_RULEFILE###

Ramps.txt:

The ramps configuration file provides the IDs of the detectors on the on-ramps, ramp length, ramp type and ramp name. The sequence of these entries is:

1. Ramp name:e.g., 36th street;
2. Ramp type:L represents local access ramp while F represents freeway to freeway ramp;
3. Queue station:TH62EB
4. Passage station: Detector ID as in freeway section e.g., 1358
5. Ramp length: Distance between queue detector and the metering pole (feet)

- The entries should be as shown below:

  String identifier: string TAB string TAB string TAB string TAB string

- No spacing after the colon;

- In case of no entry being appropriate, “none” is used as the string;

- In case of no queue detector, the ramp length needs to be set to 1 foot;

A sample ramp.txt below shows the syntax to be followed:

Sample configuration file ramp.txt
Ramp_name/type/queue_station/passage_station/ramp_length:Valley View Rd 3A1 L ValleyView 1355 350 Ramp_name/type/queue_station/passage_station/ramp_length:T.H.62 E.Bound 3A2 F TH62EB 1358 296 Ramp_name/type/queue_station/passage_station/ramp_length:T.H.62 W.Bound 3A3 F TH62WB 1361 1050 Ramp_name/type/queue_station/passage_station/ramp_length:Cedar Lake Rd 3B6 L none 1928 1

3.4 Test Sites and Data Acquisition

3.4.1. Test Site Selection Criterion

Through discussions with the Mn/DOT engineers at the TMC, three test sites were selected having geometric properties and traffic characteristics that are representative of the Twin Cities freeway network to the extent possible. The following criteria were used in choosing the sites:

I. Representative of Twin Cities freeway network

The Twin Cities freeway network includes typical geometric configurations such as weaving sections, lane drop locations, high volume entrance ramps, high volume exit ramps, etc. An effort was made to select sites which included most of these features but also avoided those that had too many weaving sections and complex geometric sections within a short span. Also, the freeways can be classified into one of the following general categories: radial, circumferential, central business district connector i.e. connecting the Minneapolis and St. Paul downtown districts. The selected sites should represent at least two of the categories.

II. Level of congestion

One of the major objectives of ramp metering is to ease freeway congestions. Test sites of various congestion levels are essential for testing ramp metering effectiveness. Hence the test sites need to be selected such that they cover at least two of three identified congestion levels, i.e., low traffic, moderately heavy traffic and very heavy traffic.

III. Representative length

The ramp metering strategy under study is the recently deployed Stratified Zone Metering. This strategy is based on dividing the freeway into zones and regulating the zone entering volumes. As described in the earlier chapter, Stratified Zone control strategy requires at least seven stations (3.0 miles) to define a complete layer. Thus, assuming a minimum of two completer layers a minimum length of 6 miles is essential.

IV. Upstream and downstream boundary conditions

If recurrent traffic congestion exists beyond the freeway segment to be simulated (i.e., either the upstream or downstream end of the freeway segment, or both, are subject to recurrent traffic congestion), essential difficulty would arise in calibrating the corresponding simulation model because the boundary conditions can not be controlled. In this case, the simulation process could deviate from what actually occurred in reality. Because of this, the sites to be selected must have the boundaries free of congestion so that the simulation model can be accurately calibrated replicating the real situation.

V. Ease of traffic data collection

As the Mn/DOT ramp metering algorithms rely heavy on real-time detector data, it is essential that the sites selected should have most of its mainline detectors in working conditions for successful calibration. In addition, all entrance and exit detectors must be operational, so that the boundary demand conditions can be well defined.

VI. Availability of alternate routes

One of the goals of this research is to have the flexibility to expand a test site(s) to include arterials associated with that freeway for future research. This would allow a study of the effects of diverted freeway-bound traffic to adjoining arterials due to ramp metering and evaluation of the impacts of ramp control on the corridor as a whole. Through information about the traffic diversion due to metering is not currently available, the selected sites have alternate routes and thus, corridor simulation is also possible once the data becomes available.

3.4.2. Test Sites

Based on the above selection criteria, two sites, i.e., TH169NB and I94EB are selected for evaluating ramp metering effectiveness in the Twin Cities metro area. These two sites are shown in Figure 3-6. Their geographical characteristics are summarized in Table 3-1.

TH 169 Northbound

The first site is a 12 mile long section of TH 169 Northbound circumferential freeway starting from the interchange with I-494 and ending at 63rd Avenue North. This mostly two lane freeway segment has 10 weaving areas, 24 entrance ramps and 25 exit ramps. Of the 17 metered ramps, 4 have HOV bypasses and 2 are freeway-to-freeway type connecting TH-62 and I-394.

I-94 Eastbound

The second site is an 11 mile long freeway section of I-94 Eastbound that connects the Central Business Districts of the Twin Cities of Minneapolis and St. Paul. Being a geometrically complex freeway, it is often severely congested during peak hours and carries heavy traffic between the two cities. It has 6 weaving areas, 3 lane drops, 19 entrance ramps (4 unmetered) and 14 exit ramps. Compared to this site, TH 169 is of medium geometric complexity and generally carries relatively lower traffic volumes.

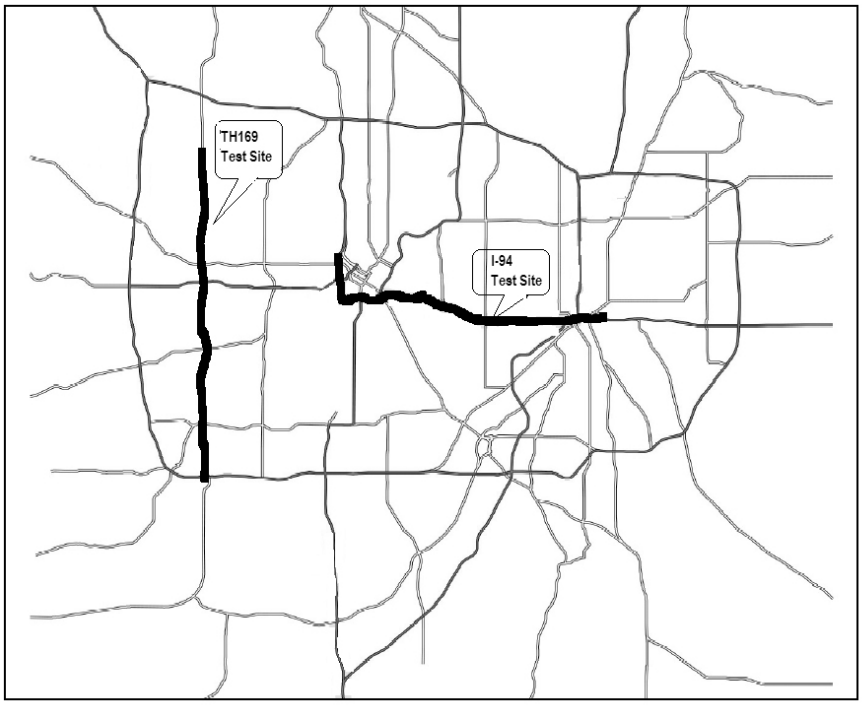

Figure 3- 6 Two Selected Test Sites: TH-169NB and I-94EB

Table 3- 1 Geometric Properties of Selected Test Sites

Characteristics	TH 169	I-94
Direction	Northbound	Eastbound
Length (miles)	12	11
Freeway Category	Circumferential	CBD Connector
Upstream Boundary	I-494 interchange	I-394 interchange
Downstream Boundary	63rd Avenue North	9th St. Off ramp
Metering Period	AM and PM	AM and PM
Metered Entrance Ramps	23	15
Unmetered Entrance Ramps	1	4
Off ramps	25	14
Weaving Sections	10	6
Lane Drop Locations	1	3
Geometric Complexity	Medium	Complex
Level of Congestion	Medium	High
Availability of Alternative Routes	No	Yes
Detector Working Conditions	Good	Good

3.4.3. Geometric Data

To create simulation models of the test sites two types of information are generally required: geometric data to model the roadway and traffic data to simulate vehicles. The geometric data consists of the physical properties of the freeway such as orientation, number of lanes, width of the lanes, length of the mainline between ramps, length of the entrance ramps, length of acceleration and deceleration lanes, location of the detectors and ramp meters, etc. The freeway alignment and orientation was obtained from the AutoCAD drawings provided by Mn/DOT in the form of centerline drawing of the entire freeway segment. These diagrams also contained the information of lane markings, and the location of traffic control devices such as detectors and ramp meters. However, to build an accurate model this data was further supplemented by aerial Digital Orthophoto Quarter-Quadrangles (DOQs). They are high resolution black and white aerial photos, 3.75' x 3.75', which cover the entire 7 county Twin Cities (Minneapolis and St. Paul) Metropolitan Area in Minnesota. They were used as background in AIMSUN to modify the simulation model to be as accurate as possible.

3.4.4. Traffic Data

The traffic detection system currently used by Mn/DOT has two components: loop detectors and closed circuit television (CCTV) cameras. Loop detectors, which form the primary component of Mn/DOT's traffic detection system, are 6' x 6' inductive loops that

are embedded in each travel lane of the freeway and placed approximately one-half mile apart on the mainline. The detectors at each location are grouped into a station. Loop detectors are also placed on all entrance and exit ramps to measure the traffic entering and leaving the freeway. The detectors on the entrance ramp are located downstream of the ramp meter and are called merge detectors. Some of the entrance ramps also have queue detectors. Each loop detector collects two types of data: volume and occupancy. Volume is a measurement of the number of vehicles that have passed over the detector. Each detector measures a lane volume and the sum of all detector volumes in a station gives the total traffic volume crossing that location. Occupancy is measured as the percentage of time during which a loop detector is occupied by a vehicle. As each detector measures the occupancy of the lane it is installed, mainline station occupancy is calculated as an average occupancy of all detectors that comprise the station. The detector station data is aggregated every 30 seconds and transmitted to the TMC whereas the individual detector data (including those on the entrance and exit ramps) is aggregated every five minutes and transmitted to the TMC.

The second type of traffic detection is through visual surveillance via CCTV cameras. The cameras are usually mounted on 50-foot poles at one mile mainline spacing and on some entrance ramps. Operators at the TMC monitor the cameras to determine if the central computer is regulating the system appropriately. They also use CCTV cameras to verify and detect freeway incidents, assist in the timely arrival of motorist aid, and help minimize traffic congestion.

An example of a mainline station (442) having two detectors (1942 and 1943) and detectors on an entrance (1944) and exit ramp (1945) is shown in Figure 6.7.

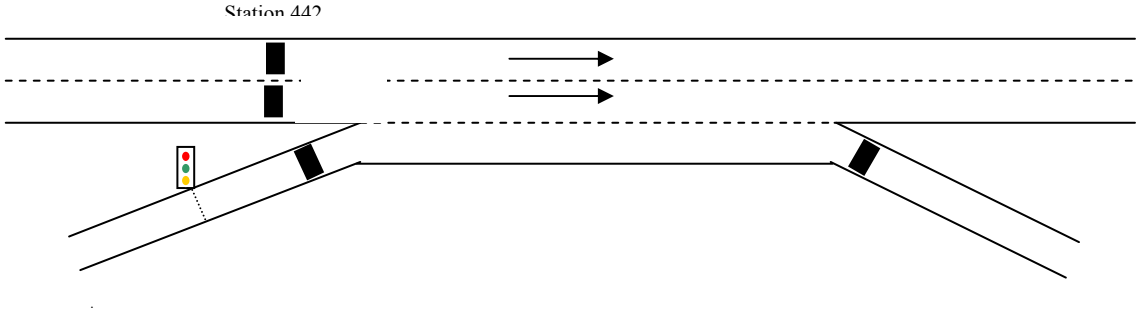

Figure 3- 7 Typical Freeway section and Loop detector locations

The traffic demand data requirements for simulation in AIMSUN are:

(1) Traffic volume and traffic composition at entrance ramps and upstream end of freeway mainline

(2) Turning percentages of mainline flow at exit ramps.

The traffic composition data, i.e., the respective percentage for each of the vehicle types constituting the traffic flow, is not available from the direct measurements of Mn/DOT traffic detecting/monitoring system. Usually, the data can be exacted from the real-time CCTV videos, supplemented by field-collected data if necessary. In particular, the traffic composition data employed for this study is the data of the year 2000. Entrance demands are retrieved from loop detector volume measurement. The queue detector located upstream of each ramp directly measures the entering demand. However, cares must be taken in checking the consistency of detector data as loop detector might malfunction and fail to give vehicle counts or occupancy. This means, the data record with a zero volume but a non-zero occupancy or vice-versa should be filtered out as the two measurements are not consistent with each other.

Turning percentages of the mainline volumes at exit ramps are important for the micro-simulator to replicate the actual traffic flow process. In this study, the turning percentage is determined from the ratio of mainline volume to exit volume. This is illustrated graphically in Figure 3.8, where the turning percentage of the mainline flow at the exit ramp is computed as:

$$P = \frac{V_{exit}}{V_{mainline}}$$

where:

P represents the turning percentage of mainline volume exiting from the off-ramp;

V_{exit} represents the volume recorded by the exit ramp detector during a prescribed time interval;

$V_{mainline}$ represents the volume recorded by the mainline detectors during a prescribed time interval.

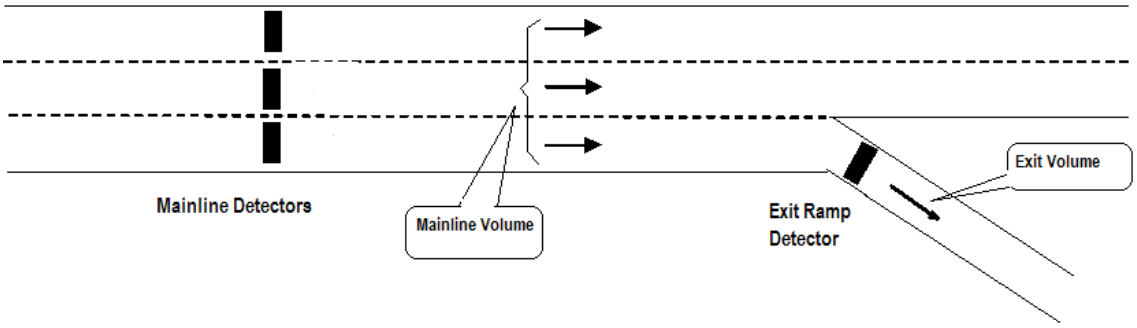

Figure 3- 8 Mainline Detectors and Exit Ramp Detector

The selected test dates are November 08, 2000 for TH-169 and November 01, 2000 for I-94. The dates were specifically selected during the ramp meter shutdown period to ensure the calibrated simulation models have no systematic bias to a particular set of control parameter values. Afternoon peak was selected as the test sites experience more severe congestion. In order to include the entire congestion cycle each simulation experiment was conducted from 14:00 to 20:00, while the SZM control period is from 15:00 to 18:00.

3.5 Simulation Model Calibration

Once the geometric and traffic data were used to build the simulation models of the test sites, the next step was to calibrate them. Simulation model calibration is the process of obtaining a good match between actual and simulated fundamental measurements (e.g., Flow and Speed) by fine tuning the global and local parameters of the microscopic simulator. In this study the calibration methodology proposed in Hourdakis and Michalopoulos, (2000) was followed resulting in very satisfactory statistical match. For instance, by comparing actual and simulated volumes on mainline detector stations, the correlation coefficient (r^2) was high ranging from 0.90-0.98 at both test sites, while similar scores were obtained for other test metrics (Thiel's coefficients, etc) and speed contours.

4. GENERAL METHODOLOGY

As mentioned in the earlier chapter, there are two major stages in the proposed performance optimization methodology; Sensitivity Analysis and Response Surface Optimization. In this chapter a general description of the methodology applicable to any ramp control strategy that has clearly defined control parameters which affect the performance of the strategy is presented. The flowchart presented in figure 4.1 summarizes the overall methodology. The following subsections present a very detailed account of this two stage methodology.

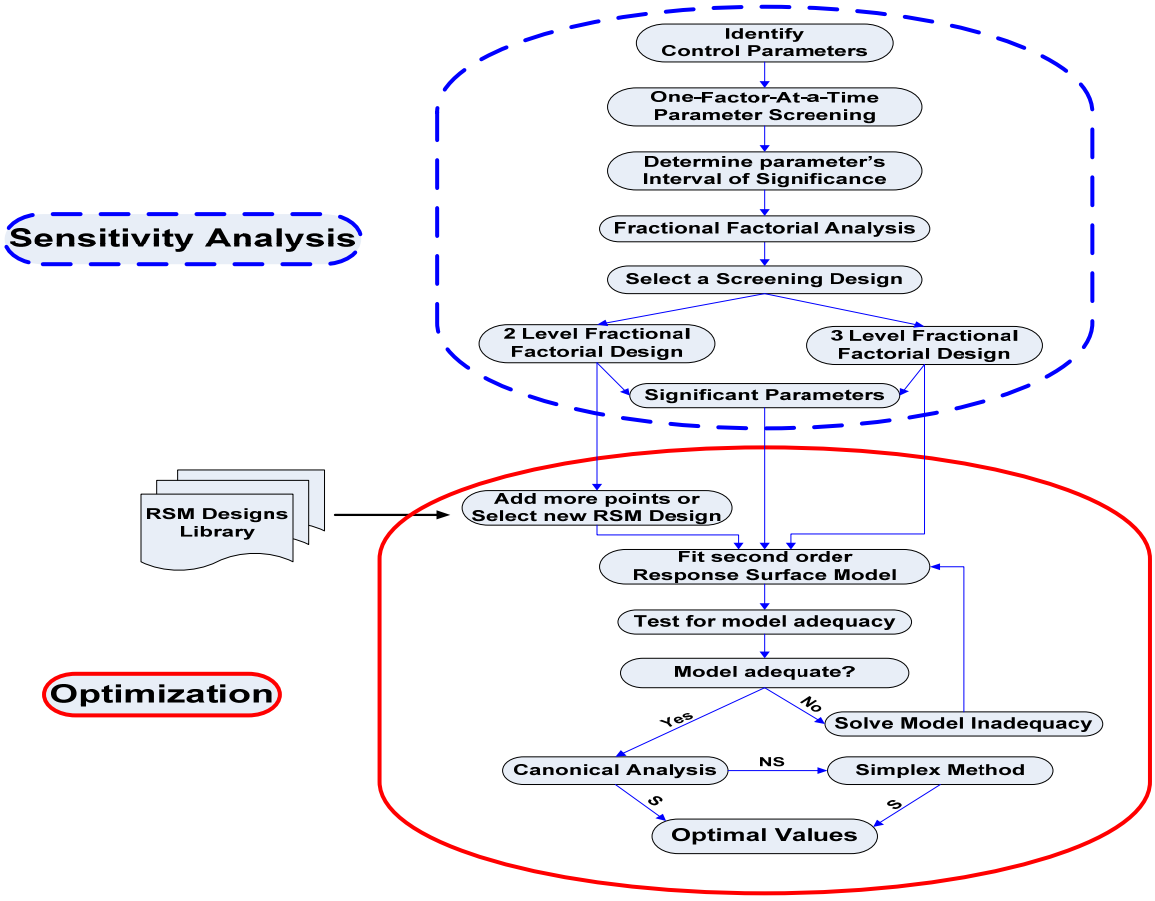

Figure 4- 1 Framework of Sensitivity analysis and Optimization

4.1 Sensitivity Analysis

Sensitivity Analysis (SA) is the study of how the variation in the output of a model (numerical or otherwise) can be apportioned, qualitatively or quantitatively, to different sources of variation. The primary purpose of a sensitivity analysis prior to optimization is to reduce the number of parameters to optimize and also the search domain. It should be noted that in the case of a small parameter set (≤ 5), sensitivity analysis becomes optional and can be skipped. However, in general this is not always the case. Thus a preliminary screening using one-factor-at a-time analysis followed by a robust analysis based on Fractional Factorial Design is employed.

4.1.1. One-Factor-At-A-Time (OFAT) analysis

OFAT sensitivity analysis, also known as threshold analysis (Critchfield and Willard, 1986), is one of the simplest ways of investigating the sensitivity of a model in the form of graphs, charts and/or surfaces. Generally, such a graphical method is used to give visual indication of how the output is affected by variations in the inputs (Geldermann and Rentz 2001).

As a first step of this preliminary sensitivity analysis, all the parameters of a control strategy and their applicable ranges are identified and a set of parameter values is selected as a reference (henceforward referred to as the base set). The method further requires defining a Sensitivity Index (e.g., percent change in MOE, rate of change in MOE). SI values are calculated by individually varying only one parameter across its range while holding all other parameters at their base values. Thus for each parameter a rough sensitivity curve is first developed using a coarse step size and if necessary is locally refined with a finer interval. A suitable threshold value of the SI is then selected and all the parameters that fall above (or below depending on the SI) are identified as most sensitive. Further, for each sensitive parameter an interval of significance is also identified.

OFAT is very useful screening technique and can expose complex dependencies between inputs and outputs (McCamly and Rudel, 1995). However, it addresses only a potentially small portion of the entire parameter domain. Further, parameter interactions are impossible to capture. Hence it is recommended here as a good practice to avoid using relatively high threshold values of SI.

4.1.2. Fractional Factorial Analysis

Factorial analysis, which is based on the principles of Design of Experiments (DOE), is an efficient approach to estimate the parameter effects and their interactions (Kleijinen, 1993 and Montgomery, 1997). It is an experimental strategy in which all parameters are varied together, instead of one at a time. Each parameter is allowed to take only a definite number of values referred to as levels. Typically a parameter is assigned not more than 5 levels. The main effect of a particular parameter is calculated as the change in response (e.g., MOE) due to a change in its level. If this difference in response between two levels of a parameter is not the same at all levels of another parameter, then the two parameters (hence forward referred to as *factors*) are said to have an *interaction*. In a full factorial analysis, all possible combinations of parameter levels are evaluated. Thus, a full factorial can estimate all two-factor and higher order interaction effects but generally needs astronomically large number of evaluations. For instance, for 10 parameters with 3 and 2 levels each will require 3^{10} and 2^{10} runs respectively. However, by reasonably assuming that higher order interactions are negligible, only a fraction of full factorial experiment is sufficient to estimate the main effects and lower order interactions. Such designs are termed as Fractional Factorial designs. The reduction in the number of evaluations is accomplished at the expense of "losing" information on main and interactions effects. This loss of information results from some main and interactions effects being entangled otherwise called "aliased" with other main and interactions effects. The effects that are entangled become inestimable as their combined effect can only be estimated from the design. The highest order of estimable interaction effects determines the Resolution of an experimental design. A design is of resolution R where no p-factor effects are aliased (or entangled) with any other effects of order less than R-p. A Roman numeral subscript is employed to denote design resolution. Thus, Resolution III designs are ones in which no main effects are aliased with any other main effect, but main effects are aliased with two-factor interactions and two-factor interactions may be aliased with each other. Resolution IV designs are the ones in which no main effect is aliased with any other main effect or with any two-factor interaction, but two-factor interactions are aliased with each other. Resolution V design are ones in which no main effect or two factor interaction is aliased with any other main or two-factor interaction, but two-factor interactions are aliased with three-factor interactions.

As it can be readily seen, the higher the resolution the better the design. However, as the resolution of design increases the number of evaluations required also increase. Therefore a good balance between loss of information and number of evaluation is required. In general, a resolution of V is considered excellent, IV adequate and III economical.

Another optional but supplementary criterion to use in search good fractional factorial designs is the minimum aberration criterion (Fries and Hunter, 1980), which is an extension of maximum resolution criterion (Box and Hunter, 1961). Technically, a minimum aberration design is defined as the design of maximum resolution which minimizes the number of pairs of aliased interactions of the crucial order. For example, a minimum aberration resolution IV design would have the minimum number of pairs of confounded interactions. Orthogonal designs allow independent estimation of all

estimable effects and also minimize the variation the regression coefficients. For the objective of this study, it is recommended to use orthogonal Resolution V designs because at least a Resolution of five is required to estimate all two factor interactions and an orthogonal design is required to ensure that both the factors and their interactions are uncorrelated. A technical description of Fractional Factorial Design construction is beyond the scope of the thesis but detailed accounts on design constructions can be found in (Box and Hunter 1961, Franklin 1984 and Suen 1997). To avoid the laborious task of constructing FF designs, the National Bureau of Standards (1957) provided a comprehensive list of design tables that were constructed based on the minimum aberration. These tables can be readily used for either 2 or 3 levels of the parameters.

Once an appropriate design is selected or constructed, for each parameter combination in the design matrix the control strategy is simulated on the test sites and performance MOEs are extracted. Using the selected MOE as a response, Analysis of Variance (ANOVA) needs to be conducted to estimate the significant main and interaction effects. Through ANOVA the null hypothesis that the parameters and their interactions have no effect on the observed responses is tested. Further relative importance of these effects can also be obtained by plotting a histogram of their standardized estimates.

4.2 Response Surface Optimization

Once the significant control parameters are identified from the above sensitivity analysis; the next stage is the actual process of optimization. Response Surface Methodology (RSM) is one of the most suitable and efficient techniques for problems where the best combination of parameters values needs to be determined. RSM is a collection of mathematical and statistical techniques for modeling and analysis of complex systems with an objective to optimize its response (Meyers and Motgomery, 1995). The methodology requires evaluations of carefully selected set of parameter combinations (known as a design) to approximate the true response of the system to lower-order polynomial models using ordinary least squares (OLS) regression. Neural networks are also sometimes used to function in the same role as polynomials models.

In this study using of second order models and selecting designs capable of estimating all the terms in the model is proposed. In the literature, a number of standard RSM designs such as Central Composite Designs, Box-Behnken Designs or D-Optimal Designs specifically developed for second order models are available. Further, many statistical analysis packages (SAS, Design Expert, JMP, MINITAB, etc) are capable of generating these design tables depending on the number of parameter making it very simple for the user. However, in case a 3 level design with a Resolution-V was used in the sensitivity analysis, the same design will be sufficient to fit a second order model and thus a standard RSM design is not required.

Typical experimental designs used in RSM are Box-Behnken designs (BBD), Central Composite designs (CCD), D-Optimal designs (DOD), 3-level full factorial designs (FLF-3) and 3-level fractional factorial designs (FRF-3). The BBD, FLF-3 and FRF-3 each requires three levels to be sampled across the region of interest of each parameter in

creating the sampling combinations. The CCD requires five levels. Both BBD and CCD are near-orthogonal with the degree of non-orthogonality changing based on the number of variables in the study. An additional design commonly used is the fractional CCD with at least resolution V. A CCD can be described as a 2-level full factorial design combined with axial runs and a center point. If the factorial portion is fractionated, the design will require fewer runs. On the other hand, Box-Behnken Designs (Box and Behnken, 1960) are built using complex combinations of two-level factorial designs and incomplete block designs. Interested reader is directed to Myers and Montgomery (1995) for a thorough explanation of all of the designs and design properties mentioned above.

One of the most important criteria for selecting a design is the number of runs required. Table 1 shows the number of runs required for each of the four designs specified versus the number of factors being investigated in the model. Note that the fractional CCD does not exist at the minimum resolution of V requirement until at least five input variables are used. Hence, the number of runs required for the fractional CCD is left blank for those three cases in the table. If k is the number of input variables in the design, then a FLF3 design requires 3^k runs. A CCD requires 2^k factorial points, 2k axial points at locations ±α along each coordinate axis with a total of $2^k + 2k + 1$ runs. Further, BBD does not exist for only two variables and has gaps in its existence due to its method of construction. The formula for the number of runs required in a BBD changes based on the number of input variables. For fractional factorial designs the plans (National Bureau of Standards, 1959), based on which the calculations are done indicated in parentheses.

It is clear from the described problem that a Full Factorial design is generally infeasible. This is also true for a full CCD by the time the number of input variables near 10. Moreover, the number of runs required should not be the only concern in selecting a design. Another concern, as mentioned earlier, is the loss of orthogonality, if any. When the columns of the design matrix are not orthogonal to each other, some degree of co linearity exists. This causes increased variance in the estimates of the model coefficients and disrupts inference on determining significant effects in the model.

Variance Inflation Factor (VIF) and Tolerance are two measures that can guide identifying Multiple Co-linearity (MC). It should be noted that the variance of the Ordinary Least Square estimator for a typical regression coefficient (say β_i) can be shown to be the following.

$$Var(\hat{\beta}_i) = \frac{\sigma^2}{S_{ii}(1 - R_i^2)}$$

where $S_{ii} = \sum_{j=1}^{n} (X_{ij} - \overline{X}_i)^2$ and R_i^2 is the unadjusted R^2 with all other explanatory variables in the model. If there is no linear relationship between X_i and the other explanatory variables in the model, then R_i^2 will be zero and the variance will be σ^2 / S_{ii}. Dividing this into the above expression for Var(β_i), we obtain the variance inflation factor and tolerance as

$$VIF(\hat{\beta}_i) = \frac{\sigma^2}{S_{ii}(1-R_i^2)} \quad \text{and} \quad \text{Tolerance} = 1/\text{VIF}$$

It is readily seen that the higher VIF or the lower the tolerance index, the higher the variance of β_i and the greater the chance of finding β_i insignificant, which means that severe MC effects are present. Thus, these measures are usually used in identifying MC. This is done by choosing each explanatory variable as the dependent variable and regress it against a constant and the remaining explanatory variables. This would thus give k–1 values for VIF. If any of them is high, then MC is indicated. However, there is no theoretical way to set a threshold value to judge that VIF is "high." In a perfectly orthogonal design matrix, each VIF would have value 1.0. As the co-linearity in the model increases the parameter VIF's also increase. Cut off values are usually used to restrict poor designs. Stating this in terms of green (g), yellow (y) and red (r) lights to relate to good, questionable and poor designs, respectively, a green light may be stated as the maximum VIF < 2 and a red light may be stated as the maximum VIF > 5 or 10. Under such a scenario, Table 4.2 categorizes the designs (Craney, 2002) listed previously in Table 4.1. An additional concern in design selection is the spacing of design points. Design points falling in a region relatively far outside or away from the rest of the data will have higher leverage in determining model coefficients. For a model with p terms and n observations (as shown in Table 1), leverage values can be determined for each design point in the design matrix. Thus, average leverage equals the number of model terms divided by the number of experiments, i.e., p/n. Higher leverage points, those with values twice that of the average will unduly influence the model fit. So, designs with maximum leverages less than 2p/n are considered a green light and designs with maximum leverages greater than 4p/n are considered a red light. Values in between are in the yellow light region. Under these considerations, along with 2p/n and 4p/n limits, the above designs are presented in Table 3. Of the designs mentioned, leverages seem to be of concern mainly in the CCD. The axial points that extend beyond the face of the cube are an increasing function of the number of points required to make up the factorial portion of the design. To maintain rotatablilty, which ensures constant prediction variance at all points that are equidistant from the center in the design space, a CCD requires that its axial points must be at $\pm\sqrt[4]{n_f}$, where n_f is the number of points comprising the factorial portion of the design. Using the information provided in Tables 2 and 3, an appropriate design can be selected prior to evaluations and fitting a model. If we look at the tables 1, 2 and 3 simultaneously, we can infer that the type of design to be selected largely depends on the number of factors involved. Moreover, depending on the balance between efficient and economical designs that an experimenter is desired to seek, the class of design that is appropriate differs. Overall, Fractional CCD and Fractional Factorial Designs seem to be generally promising and BBD's are usable for 3-7 parameters. In the objective of this study, a fractional factorial design (as provided by National Bureau of Standards (1959)) is proposed, even though they are the most economical, as they are complete orthogonal designs and also nearly rotatable (refer figure 5-3).

After selecting an appropriate and all the design points are simulated in the microscopic simulator, a response surface model is fit to the data using least squares regression. However, it is worth noting that the response data is not truly a random variable. If a combination of parameters is simulated more than once, keeping the random seeds the same, the average response returned by the simulator will repeat itself exactly. Thus, lack of fit tests are not possible in simulation based RSM and the replications need not be used for any of the points in this process, including the center points if any. The model fitting process is unaffected by this information. However, the concern for validation of standard assumptions for the residuals that they are independent and identically distributed, iid N $(0, \sigma^2)$ needs to be addressed. The three main underlying assumptions of iid are: 1) Normally distributed residuals symmetric about zero mean with the majority of the data close to zero; 2) Homoscedastic residuals exhibiting a constant variance throughout the range and with no clear curvature in Residulas vs Predicted plot; 3) No Outliers with all observations falling within a maximum allowed Cook's Distance of 4/(n-k-1), where n is the number of observations and k is the number of parameters.

However, goodness of fit is determined based on indirect checks. The principal statistical criterion that determines the goodness of fit is R^2, the coefficient of determination. The modeling technique need not be based on data from a random variable, but a good fit of the model to the data is still evidence that the response surface model adequately replaces the simulation model. The model validation methods mentioned above are all criteria of a statistically good model.

With diagnostic checking and model adequacy tests are conducted ensuring that the fitted second order model is statistically valid, response surface analysis needs to be performed. Canonical Analysis is basis for determining the location and the nature of the stationary point (X_0) of the model. The estimated second order approximation of the simulation model for the selected MOE can be written as follows:

$$\hat{y} = \hat{\beta}_0 + X'b + X'BX$$

$$x = \begin{bmatrix} x_1 \\ x_2 \\ . \\ . \\ x_k \end{bmatrix} \qquad b = \begin{bmatrix} \beta_1 \\ \beta_2 \\ . \\ . \\ \beta_k \end{bmatrix} \qquad B = \begin{bmatrix} \hat{\beta}_{11} & \hat{\beta}_{12}/2 & . & . & \hat{\beta}_{1k}/2 \\ & \hat{\beta}_{22} & . & . & \hat{\beta}_{2k}/2 \\ & & . & . & . \\ & & & . & . \\ sym & & & & \hat{\beta}_{kk} \end{bmatrix}$$

$$X_0 = -\frac{1}{2} B^{-1} b$$

The nature of the stationary point is determined from the sign of the eigervalue of the matrix *B*. Relative magnitude of these eigenvalues can be helpful in overall interpretation. Let E be the matrix of normalized eigenvectors of *B* and $v_{1,}...v_k$ be the eigenvalues of B. If all eigenvalues are positive (negative), then the quadratic surface has a minimum

(maximum) at the stationary point (X_0). If the eigenvalues are mixed in sign, then the stationary is a saddle point. It is not advisable to extrapolate the second order models beyond the current region of interest (Myers and Montgomery, 1995). Therefore, if the stationary point (minimum, maximum or saddle point) lies outside the current region of interest, the stationary point is not accepted. In such a case a numerical optimization of the response surface is performed using algorithms like Newton Method and Nelder and Mead Simplex method.

Graphical analysis plays an important role in illustrating and interpreting the RSM in the form of contour and perturbation plots. The Contour plots are two-dimensional graphs that show constant response curves with the axis system being a specific pair of parameters while all others are held constant. These plots are particularly revealing when the stationary point not of practical significance, which is usually the case. On the other hand , perturbation plots help compare the effect of all the parameters at a particular point in the RSM design space. The response is plotted by changing only one parameter over its range, while all other parameters are fixed at user desired values.

Many advanced statistical packages (JMP, Design Expert, SAS, MINITAB, SPSS, etc.) have the ability to perform RSM optimization and have built-in standard designs as mentioned earlier, making it simple for the user to implement this methodology. Further, contour plots, perturbation plots can also be easily obtained in most of these packages. For this study, while Design Expert® 6 has been the chief tool for modeling and analysis of RSM, SAS® has been used to conduct canonical analysis as this feature is unavailable in Design Expert®.

Table 4- 1 Number of runs required by type of Design for RSM

No: Factors	BBD	CCD	Fractional CCD (Min. Res. V)	Full Factorial Design	Fractional Factorial Design (Min. Res. V)
2	-	9	-	9	-
3	13	15	-	27	-
4	25	25	-	81	-
5	41	43	27	243	81 (3.5.3)
6	49	77	45	729	243 (3.6.9)
7	57	143	79	2187	243 (9.7.9)
8	-	273	81	6561	243 (27.8.9)
9	121	531	147	19,683	243 (81.9.9)
10	161	1045	149	59,049	243 (243.10.9)
11	177	2071	151	177,147	243 (729.11.9)
12	193	4121	281	531,441	729 (729.12.27)

Table 4- 2 Classification of Designs for RSM with respect to Maximum VIF

No: of Factors	BBD	CCD	Fractional CCD (Min. Res. V)	Full Factorial Design	Fractional Factorial Design (Min. Res. V)
2	-	1.68 (g)	-	1.00 (g)	-
3	1.35(y)	1.91 (g)	-	1.00 (g)	-
4	2.21 (y)	2.21 (y)	-	1.00 (g)	-
5	3.15 (y)	2.44 (y)	1.67 (g)	1.00 (g)	1.00 (g)
6	2.32 (y)	2.07 (y)	2.25 (y)	1.00 (g)	1.00 (g)
7	2.32 (y)	1.53 (g)	2.52 (y)	1.00 (g)	1.00 (g)
8	-	1.24 (g)	2.56 (y)	1.00 (g)	1.00 (g)
9	3.87 (y)	1.11 (g)	2.15 (y)	1.00 (g)	1.00 (g)
10	3.69 (y)	1.05 (g)	2.56 (y)	1.00 (g)	1.00 (g)
11	2.59 (y)	1.03 (g)	2.73 (y)	1.00 (g)	1.00 (g)
12	3.63 (y)	1.01 (g)	1.79 (g)	1.00 (g)	1.00 (g)

Table 4- 3 Classification of Designs for RSM with respect to Maximum Leverage

# Input Variables	Box-Behnken	CCD	Fractional CCD (min. Res. V)	3-Level Full Factorial
2	-	1.00 {1.33,2.67} (g)	-	0.81 {1.33,2.67} (g)
3	1.00 {1.54,3.08} (g)	0.99 {1.33,2.67} (g)	-	0.51 {0.74,1.48} (g)
4	1.00 {1.20,2.40} (g)	1.00 {1.20,2.40} (g)	-	0.28 {0.37,0.74} (g)
5	1.00 {1.02,2.05} (g)	0.89 {0.98,1.95} (g)	0.88 {1.56,3.11} (g)	0.14 {0.17,0.35} (g)
6	1.00 {1.14,2.29} (g)	0.57 {0.73,1.45} (g)	0.97 {1.24,2.49} (g)	0.06 {0.08,0.15} (g)
7	1.00 {1.26,2.53} (g)	0.56 {0.50,1.01} (y)	0.82 {0.91,1.82} (g)	0.0285 {0.033,0.066} (g)
8	-	0.55 {0.33,0.66} (y)	1.00 {1.11,2.22} (g)	0.0122 {0.014,0.027} (g)
9	1.00 {0.91,1.82} (y)	0.54 {0.21,0.41} (r)	0.55 {0.75,1.50} (g)	0.0051 {0.006,0.011} (g)
10	1.00 {0.82,1.64} (y)	0.53 {0.13,0.25} (r)	0.78 {0.89,1.77} (g)	0.0021 {0.0022,0.004} (g)
11	1.00 {0.88,1.76} (y)	0.52 {0.08,0.15} (r)	0.99 {1.03,2.07} (g)	0.0008 {0.0009,0.002} (g)
12	1.00 {0.94,1.89} (y)	0.52 {0.04,0.09} (r)	0.54 {0.65,1.30} (g)	0.000326 {0.00034,0.00068} (g)

5. IMPLEMENTATION TO SZM CONTROL STRATEGY

5.1 OFAT Analysis

The SZM control has twenty parameters as described in the Table 5.1. Throughout this study, the parameter values that are currently being used by Mn/DOT are considered as base values. Henceforward it is implicitly understood that this set defines the base case for all comparisons. As mentioned earlier, the primary MOE selected for this study was System Total Travel Time (STTT). Using percentage decrease in STTT from base case as a sensitivity index (SI), the sensitivity curves (rough or fine as required) were developed for all the parameters at both test sites TH-169 and I-94. A small threshold value of 0.5% was used to screen the parameters.

In spite of this seemingly small threshold most parameters were found insignificant leaving only nine significantly contributing to performance. Table 5.2 shows the intervals of significance of these parameters and the three levels (-1, 0, 1) selected for the further analysis. As expected, the sensitivity curves suggest that the control performance is non-linearly related to its parameters. For TH-169 and I-94 most of the curves exhibited similar overall trends, but their intervals of significance were shifted. This justified the need for a site specific optimization of the control parameters.

Capacity estimates for the mainline (rightmost and other lanes), Maximum ramp waiting time threshold, Absolute Max. Release rate, etc strongly affect the system performance. Among the less sensitive parameters are the smoothing constants (for metered and unmetered ramp demand, mainline flow rate, etc.), Absolute Min. ramp release rate, etc. The following section explains the effects of changes in all the screened parameters and their observed trends in OFAT sensitivity analysis. Percent changes in System TTT, Mainline TTT and Ramp TTT from the base are plotted for both test sites with a base value of parameter being represented as a short vertical line.

Table 5- 1 SZM Control parameters and their applicable ranges

No:	SZM Control Parameter	Notation	Units	Current Value	Applicable Range
1	Absolute Maximum Release Rate	R_{max}	Veh/hr	1714	1300 - 1714
2	Absolute Minimum Release Rate	R_{min}	Veh/hr	240	180 - 360
3	Increment to ramp demand	I_{ramp}	Veh/hr	150	80 - 240
4	Full Density of a zone	D_f	Veh/mile	32	23 - 40
5	Max. Allowed waiting time on Local ramps	$T_{max,\,L}$	Seconds	240	180 - 530
6	Max. Allowed waiting time on F-F ramps	$T_{max,F}$	Seconds	120	80 - 240
7	Queue Density equation-Intercept	$Q_{Intrecept}$	Veh/mile	206.715	200 - 240
8	Queue Density equation-Slope	Q_{Slope}	Hr/mile	0.03445	0.02 - 0.06
9	Capacity Estimate for Rightmost mainline lane	C_R	Veh/hr	1800	1700 - 2200
10	Capacity Estimate for Other mainline lanes	C_O	Veh/hr	2100	1800 - 3000
11	Occupancy Threshold	O_{Th}	%	25	12 - 46
12	Ramp Meter Turn off threshold	M_{off}	%	80	50 - 80
13	Ramp Meter Turn on threshold	M_{on}	%	85	50 - 100
14	Passage Compensate Factor	P_c	-	1.15	1.00 - 1.5
15	Accumulate Release rate smoothing factor	K_R	-	0.20	0.1 - 0.7
16	Queue Detector smoothing factor	K_D	-	0.15	0.1 - 0.7
17	Passage Detector smoothing factor	K_P	-	0.20	0.1 - 0.7
18	Mainline station smoothing factor	K_M	-	0.15	0.1 - 0.7
19	Unmetered station smoothing factor	K_U	-	0.15	0.1 - 0.7
20	Exit station smoothing factor	K_X	-	0.15	0.1 - 0.7

Table 5- 2 Screened SZM Parameters and Levels in Interval of Significance

No:	Parameters for FF Design	Notation	Units	Factor Code	†Levels for TH169			†Levels for I94		
					-1	0	1	-1	0	1
1	Absolute Maximum Release Rate	R_{max}	Veh/hr	A	1540	1600	1660	1400	1520	1640
2	Occupancy Threshold	O_{Th}	%	B	20	30	40	20	30	40
3	Increment to Ramp demand	I_{ramp}	Veh/hr	C	120	150	180	150	180	210
4	Passage Compensate factor	I_{ramp}	Veh/hr	D	1.2	1.3	1.4	1.2	1.3	1.4
5	Ramp Meter Turn on Threshold	P_c	-	E	0.7	0.8	0.9	0.7	0.8	0.9
6	Capacity Estimate for Rightmost mainline lane	C_R	Veh/hr	F	1800	1950	2100	1750	1900	2050
7	Capacity Estimate for Other mainline lanes	C_O	Veh/hr	G	2100	2400	2700	2100	2400	2700
8	Full Density of a zone	D_f	Veh/mile	H	30	35	40	25	30	35
9	Max. Allowed waiting time on Local ramps	$T_{max,\,L}$	Second	J	240	330	420	300	390	480

5.1.1. Parameter Sensitivity Curves

Maximum Release Rate (R_{max}):

In the Twin Cities metro area, it has been a standard to meter ramps only if two or more storage lanes can be provided. In Dual-lane metering the controller operates by alternating the green-yellow-red cycle for each lane. Depending on the controller being used the cycle may or may not be synchronized. In the twin cities synchronized controlled ramps are designed to two lanes before the ramp meter but transitioned into one lane before merging the freeway. From a practical point of view, for a single lane ramp with one vehicle per green the smallest possible cycle is 4 seconds with 1 second green, 1 second yellow and 2 seconds red. This produces a maximum ramp release rate of 900 VPH. On the same lines, dual lane metering can provide a metering capacity of 1600 to 1700 VPH. The value currently used by MN/DOT is 1714 VPH which corresponds to a cycle time of 2.1 seconds (2 seconds for yellow plus green and 0.1 second for red). As any smaller cycle length than 2.1 seconds will be infeasible to drivers, the tested range of this parameter was from 1714 VPH to 1300 VPH. The sensitivity curves for both the test sites show that as R_{max} decreases from its base value Ramp TTT increases steadily as fewer and fewer vehicles are allowed to enter the mainline. However, Mainline TTT and System TTT are affected non-linearly with minimum mainline TTT occurring when R_{max} is in the neighborhood of 1600 and 1400 VPH for Th169 and I94 respectively. A lower value for I-94 can be attributed to the fact that it is more severely congested test site with the maximum release rate of a ramp depends on the test site and the congestion level.

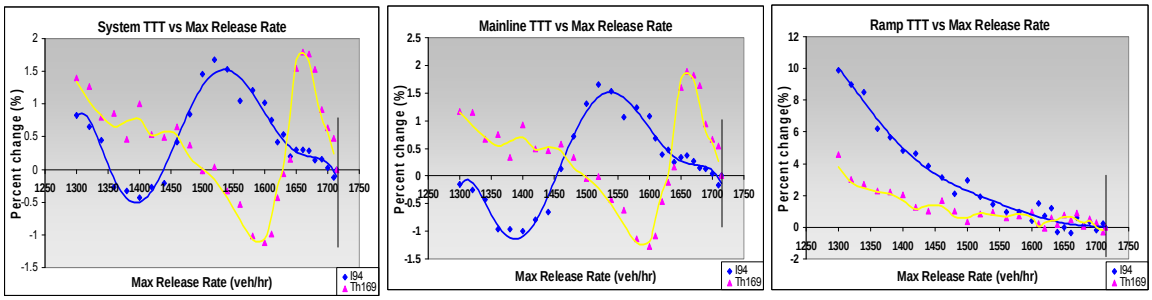

Figure 5- 1 Effect of parameter Max Release Rate on Performance MOEs

Occupancy Threshold *(O_{Th}):*

Occupancy threshold is a control parameter that detects queues with the back of the queue approaching a queue detector. As this threshold increases, the theoretical storage space on a ramp increases thereby allowing larger queues and consequently high Ramp TTT. The current value of 25% used in SZM control is equivalent to an average density *($d = O_s * 52.80 / L_e$)* of 53 veh / mile. For both the test sites similar overall trend was observed. As expected, RTTT increases sharply from with the threshold value increasing

from 15 % to 30% and then flattens between 30 % and 45%. However, STTT and MTTT decrease as O_{Th} changes from 20% to 30% and then increase when O_{Th} changes from 30% to 45%.

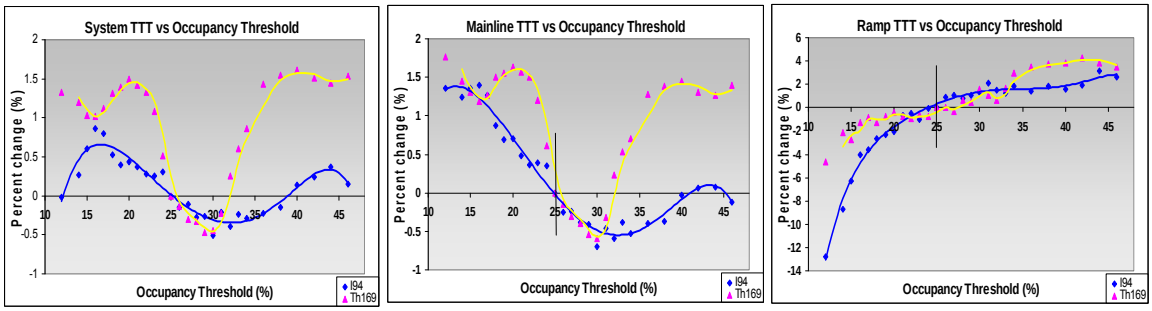

Figure 5- 2 Effect of parameter Occupancy Threshold on Performance MOEs

Increment in Ramp Demand *(I_{Ramp}):*

When a ramp queue exceeds beyond the queue detector, the detector counts are no more accurate. To avoid such a condition, whenever the queue detector occupancy increases a predetermined threshold, ramp demand is increased by $\boldsymbol{I_{Ramp}}$ veh/hr for the next control period. Clearly for a given occupancy threshold as the value of this control parameter increases, the storage space available for the ramp queue decreases. Thus, the Ramp TTT decreases steadily. However, the effect on Mainline and System TTT is non-linear and also depends on the congestion level on the freeway. On the moderately congested site TH169 at lower increment values the MTTT like s the mainline TTT increases

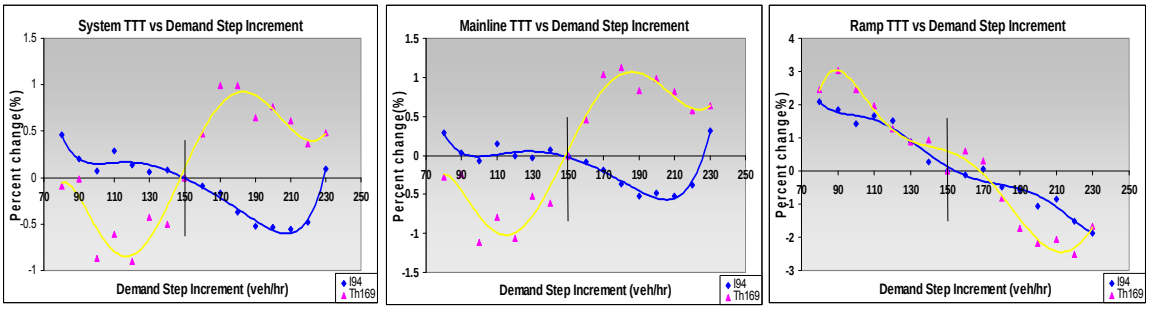

Figure 5- 3 Effect of parameter Ramp demand Increment on Performance MOEs

Capacity Estimates *(C_R & C_O):*

Capacity estimates of rightmost lane and all other lanes are two parameters which are used in the determining the downstream mainline capacity of a zone (B). According to *Highway Capacity Manual* (HCM, 2000), the capacity of a freeway section should not be

more than 2200 vphpl when the free flow speed is 65 mph. However, recent studies on the stochastic nature of freeway capacity (Polus and Pollatschek, 2002 and Persaud, 2001)) have shown that probability density function of freeway capacity follow shifted gamma distribution. The capacity of the rightmost lane is considerably lower than that of the middle lane which is also lower than the leftmost lane (assuming a 3-lane freeway section). The flows of the highest probability occur at 2100 veh/hr, 2375 veh/hr and 2800 veh/ hr on the rightmost, middle and left most lanes (Polus and Pollatschek, 2002). Moreover, very high flows up to 3000 veh/hr can also be reached on left most lanes but with very low probabilities. Thus, in this study a wide range of values was tested; a range of 1700 veh/hr to 2250 veh/hr for right most lanes and a range of 1800 veh/hr to 3000 veh/hr for other lanes were considered for the two parameters C_R and C_O.

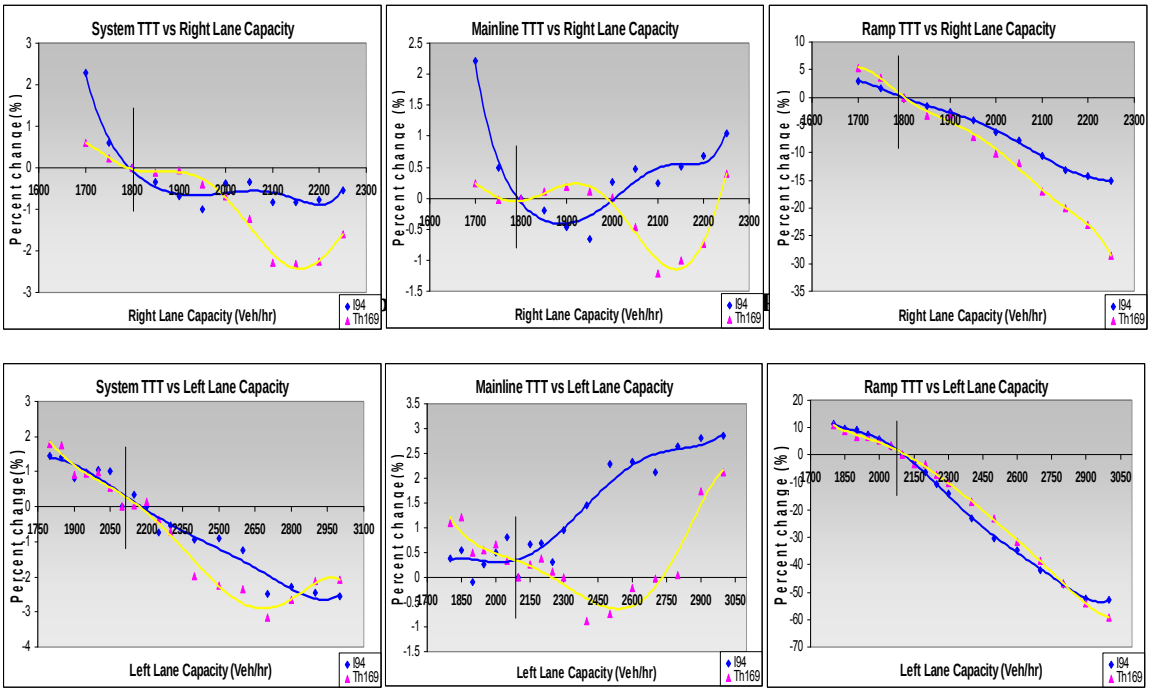

Figure 5- 5 Effect of parameter Other-lane capacity on Performance MOEs

The sensitivity curves show that as the capacity estimates of right and other lanes increase the total allowed metered ramp flow increases in every zone. Thereby, less and less restrictive ramp release rates will be proposed resulting in lower ramp waiting time and Ramp TTT. This can be clearly noted as the case on both test sites irrespective of the level of congestion on the freeway. However, the effect on the mainline, and thus also on the system, differs significantly between the TH-169 and I-94. Figure 5.4 shows that the mainline of a moderately congested site like TH-169 can accommodate higher C_R values than its current default of 1800 veh/hr but will eventually deteriorate at values higher than 2100 veh/hr. On the other hand I-94 being a congested freeway, its mainline TTT starts to shoot up at a much lower C_R value of 1900 veh/hr as compared to TH-169. The system TTT decreases initially up to a C_R value of 2100 veh/hr and then increases sharply.

The effect of other lane capacity estimate C_O on the performance MOEs is similar to that of rightmost lane estimate C_R. However it has stronger effect as this estimate is used for more than one lane in a zone as compared to C_R. TH-169 has mostly 2-lane freeway sections but out of 12 miles more than 4 miles is 3-lane. I-94 is a mostly 3-lane freeway with some 4 and 5 lane sections. Being already congested, mainline of I-94 deteriorates for any value higher than the current default value of 2100 veh/hr. But, large improvements in RTTT offset this increase in MTTT, thereby improving the STTT. This is also consistent with TH-169, except that the between mainline performs better than the base scenario in between 2300 veh/hr and 2700 veh/hr.

Maximum Allowed Ramp Waiting Time *(T_{max}):*

T_{max} is the main control parameter that governs the queue control policy in SZM. In any case, the control logic maintains that the last vehicle in the estimated queue on a ramp is released within T_{max} . The current default value of T_{max} is 4 minutes (240 seconds) for all local access ramps. A wide range (180-520 sec) of this parameter was tested to capture its effect on all the three selected MOEs as shown in Figure 5.5. Ramp TTT keeps increasing with increase in Tmax and it tends to reach a state where the ramps do not get any worse. However, this state occurred at two different values of Tmax , 420 seconds and 480 seconds on TH-169 and I-94 respectively. In the case of Mainline TTT, TH-169 improves steadily as Tmax is changed from 180 to 420 seconds, but further the improvements are marginal. In the case of I-94, which carries heavier volumes of traffic, similar trends are observed but with a lower improvement and at a higher cost of total waiting time on the ramps. Overall, the System TTT of I-94 increases with T_{max} as the mainline improvements are offset by the increase in the Ramp TTT. However, TH-169 exhibits considerable decrease in System TTT between the values 240 and 420 as shown in Figure 5.6.

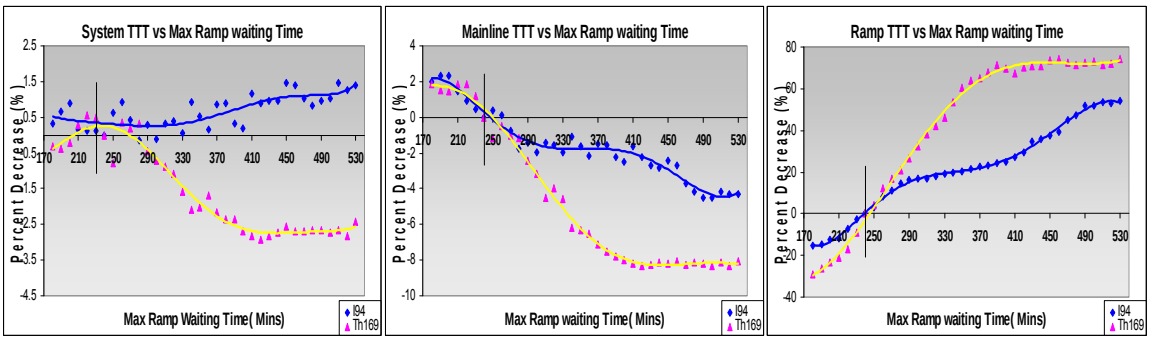

Figure 5- 6 Effect of Maximum ramp waiting time on Performance MOEs

Full Density of a Zone *(D_f):*

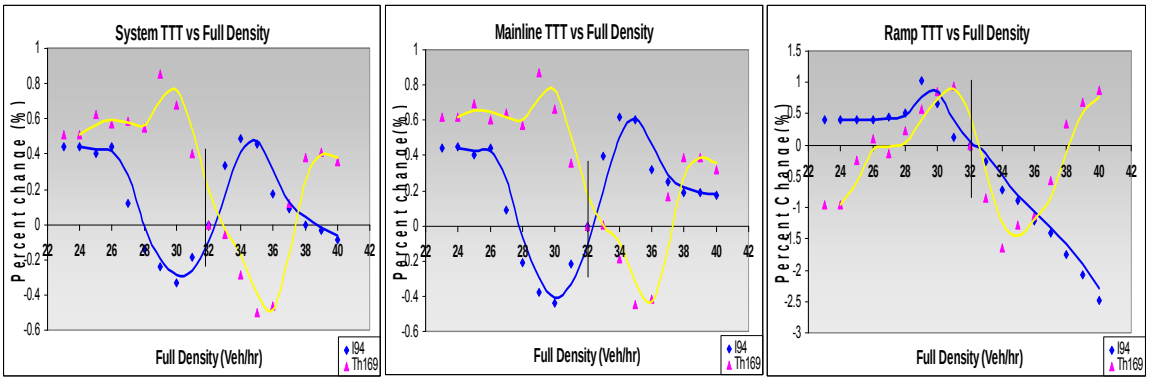

Figure 5- 7 Effect of parameter Full density on Performance MOEs

The parameter full density of a zone reflects the available space within a zone. The current default value is 32 veh/mile (corresponds to 15% occupancy). As the parameter value increases more spare capacity on the freeway is available. Thus the RTTT continues to decrease. Mainline and System TTT of I-94 is unaffected small values of $\boldsymbol{D_f}$. However in the interval between 26 and 40 a minimum and a maximum occurs. TH169 also has exhibits similar trend but with a shifted interval of 30 and 40. Minimum STTT and MTTT occur at a higher value of $\boldsymbol{D_f}$ (~ 36 veh/mile) in the case of TH169. This is because of the low densities on the mainline of TH169 which helps the SZM control to allow more vehicles to merge from the ramps.

Passage Compensation Factor *(P_c):*

In the absence of a queue detector, which is sometimes the case, a passage detector is used to replace the queue detector measurements. However, as mentioned earlier, these counts do not represent the true ramp demand. Thus, this empirical parameter compensates for the error by multiplying counts of the passage detector by a factor greater than 1.0. The current default value is 1.1. The range of values that were tested for $\boldsymbol{P_c}$ is between 1.0 and 1.5. As both the sites have situations where a queue detector is missing, very similar trends were observed. Clearly, RTTT is affected strongly as it decreases with increase in $\boldsymbol{P_c}$**.** Mainline TTT and System TTT experience minimum values at an approximate value of 1.3. Thus, an interval of 1.2 -1.4 was selected for next stage of analysis.

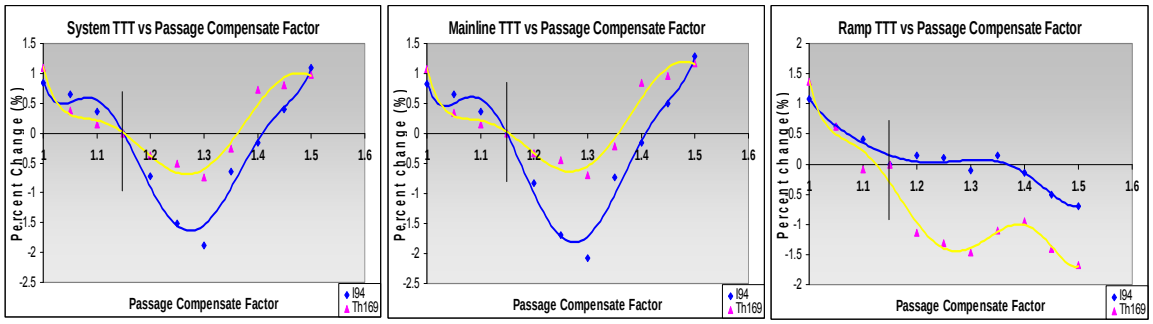

Figure 5- 8 Effect of Passage compensate factor on Performance MOEs

Ramp Meter Turn-on threshold *(M_{on})*

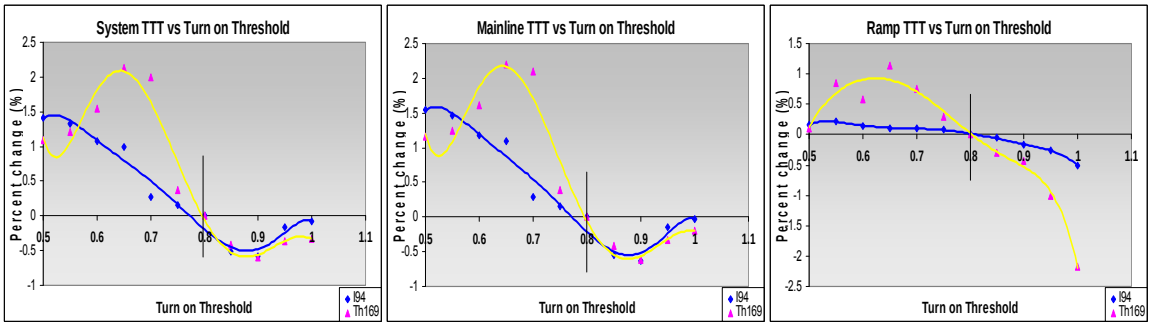

Figure 5- 9 Effect of parameter Turn-on threshold on Performance MOEs

Even before ramp meters begin operating an accumulated release rate (R_a) is calculated from the release rates proposed by the algorithm. After the start time, a meter will begin operation when the ramp demand is greater than $\boldsymbol{M_{on}}$ times the accumulated release rate. This is to ensure that the ramp demand is high enough to warranty metering. Thus, in this experiment $\boldsymbol{M_{on}}$ had been tested over a range of 0.5 to 1.0, while the current default value is 0.80. The plots in Figure 5.9 show that operating at a slightly higher threshold than the present practice will produce improvements in all the performance MOEs. This is consistent with both the test sites.

5.2 Fractional Factorial Analysis

Considering the nonlinearity of the sensitivity curves, in order to capture the curvature effects three levels are selected for each parameter within its interval of significance. Thus for 9 parameters a full factorial would have required 3^9 (=19683) evaluations. With a 3_V^{9-4} Fractional Factorial Design the number of evaluations is reduced to 243, which is only a 1/81 fraction of the full factorial. The selected design is orthogonal and has a resolution V (refer Appendix A). With 10 replications at each design point, for each site the whole experiment required 250 computer hours (~10 days) on a Pentium PC.

5.2.1. Significant Parameters and Interactions

The results from ANOVA with System TTT as response were obtained for the two test sites. It should be noted that ANOVA has to be conducted on standardized parameters with their levels coded between -1 and 1 as shown in Table 5.2. Figure 4 illustrates the relative importance of the nine control parameters and their interactions using their coefficient estimates in the ANOVA. The analysis shows that the Capacity estimate for the rightmost lane (F), Capacity estimate for other lanes (G) and Maximum allowed ramp waiting Time (J) are highly significant to system performance of SZM control. Moreover, they exhibit strong mutual interactions. Hence, the choice of these parameter values is not trivial and only specific combinations might produce an optimal performance. Further, G and J also exhibit quadratic effects. Among the other parameters, Maximum release rate (A), Occupancy Threshold (B) and Meter Turn on Threshold (E) are also statistically very significant depending on the test site. Moreover, it is worth noting that at 90% confidence level all the parameters are found significant in either directly as a main effect or in the form of an interaction with other main effects. Therefore, all parameters are considered significant and so should be included in the next step, performance optimization by RSM.

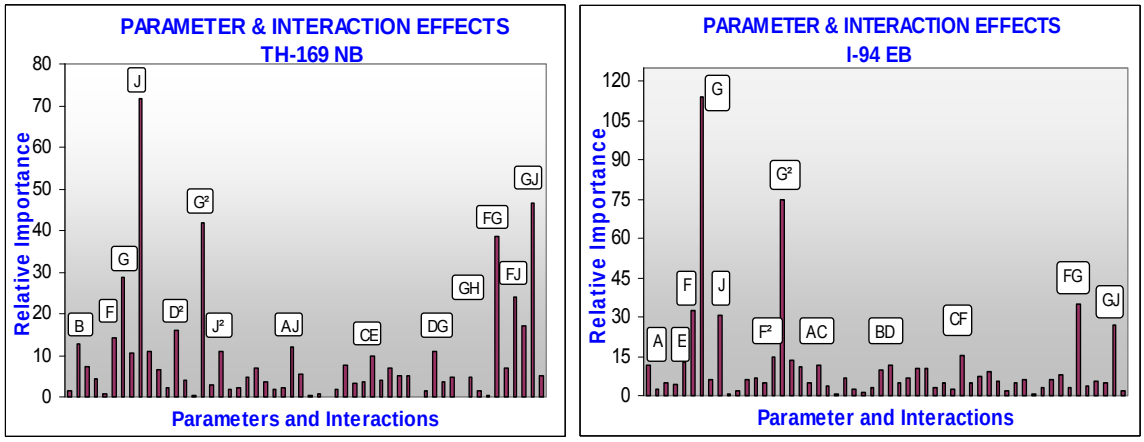

Figure 5- 10 Standardized Parameter and Interaction Effects on STTT

5.3 Response Surface Model Fitting and Optimization

As mentioned in the earlier chapter, optimization by RSM requires selection or construction of an appropriate design that satisfies certain design criteria. From the fractional factorial analysis of SZM control, it has been concluded that all the nine parameters should be included in the performance optimization. Further, it needs to be

noted that the 3_V^{9-4} fractional factorial design used in the Fractional Factorial analysis is also capable and indeed one of the preferred designs in estimating not only the main effects and interactions but also the quadratic effects. Thus, the same design was used to fit the second order model in nine parameters. This is an orthogonal and resolution V design. Moreover, the shape of the standard error plot of a design reveals its nature. Figure 5.1 is the 3-D view of the standard error plot of the selected 3_V^{9-4} fractional factorial design which shows a nearly circular and a symmetric 3-D shape. This is a feature of nearly rotatable designs. Further, the plot also shows relatively low and flat error near the central region.

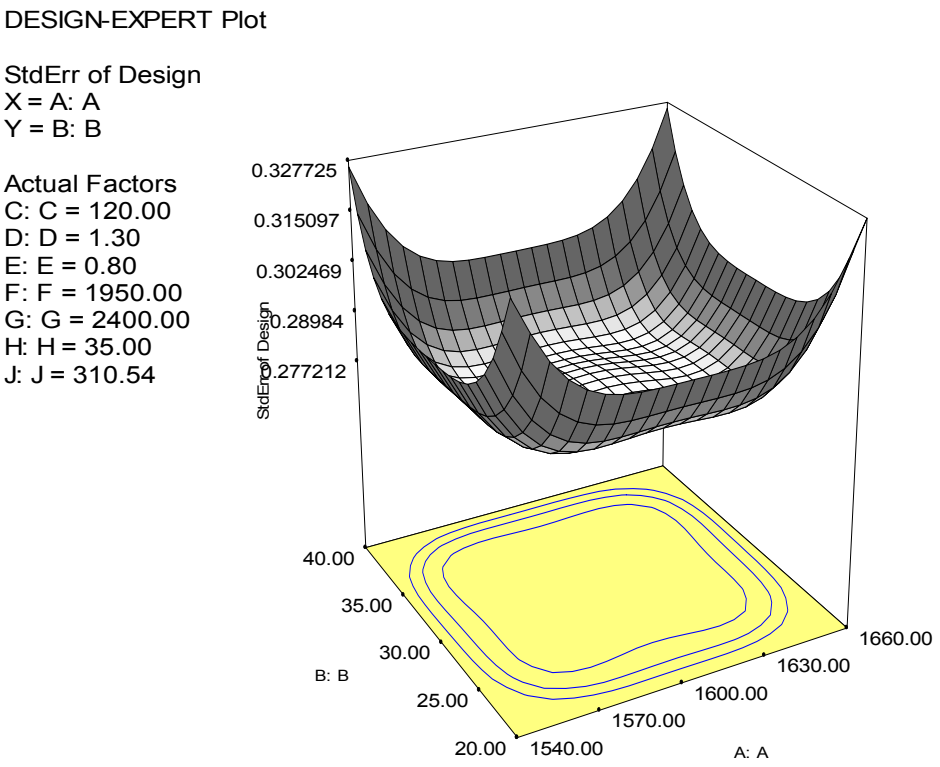

Figure 5- 11 3_V^{9-4} Fractional Factorial Design Standard Error Plot: 3D View

The model fitting, analysis and optimization was performed using Design Expert® 6, statistical software for design of experiments [Stat-Ease, 2003]. Design Expert® does not provide the feature of canonical analysis. SAS® has been used for this analysis. However, in Canonical analysis of Response Surface models is conducted in SAS®. However, in none of the cases the stationary point is found within the feasible region. This is generally the case with response surfaces involving many dependent variables. Thus, numerical optimization is opted for. Numerical optimization in Design Expert® is based on Nelder and Mead Downhill Simplex multi-dimensional pattern search (Nelder., 1965). Description of the algorithm is outside the scope of this thesis as proposed methodology

does not necessarily require this algorithm only. Any efficient optimization algorithm can replace this Simplex search technique.

A major advantage of RSM is its ability to use only one set of evaluations to independently model and optimize as many outputs as generated from the system. In the present case, the outputs are the selected performance MOEs of SZM Control. Thus, all the three selected MOEs: System TTT, Mainline TTT and Ramp TTT were modeled and optimized individually. Besides, for each MOE two scenarios were identified. These two cases arise from a specification by Mn/DOT to maintain one of the most important parameters of the algorithm, the Maximum allowed ramp wait time *(T_{max})*, equal to 4 minutes. Thus, Scenario 1 refers to Optimization with 'T_{max} free to vary' while Scenario 2 refers to Optimization with 'T_{max} set to 4 minutes'.

5.4 Results

5.4.1. Model Results

The General form of the developed second order models is:

$$y = \beta_0 + \sum_{i=1}^{k} \beta_i x_i + \sum_{i}^{k} \beta_{ii} x_i^2 + \sum \sum_{i<j} \beta_{ij} x_i x_j$$

Where, y = System TTT, Mainline TTT or Ramp TTT

x_i = Parameter$_i$

k = 9 for scenario 1

= 8 for scenario 2

These general models were simplified based on Backward Elimination (Cook and Weisberg, 1999) of insignificant terms with model hierarchy being maintained. A well-formatted model will maintain hierarchy and will include all main effects present in the significant interactions. Thus, for each test site 6 simplified models were developed and the corresponding optimal values were obtained using numerical optimization in the Design Expert® software. The following tables present the models and the degree of significance of the terms in these simplified models. Tables 6.1, 6.2 and 6.3 correspond to System TTT, Mainline TTT and Ramp TTT models of TH69. Similarly, Tables 6.4, 6.5 and 6.6 correspond to System TTT, Mainline TTT and Ramp TTT models of I94.

Table 5- 3 Simplified Response Surface Model of TH-169 System TTT

TH-169:

Term	Coefficient		P-value	Term	Coefficient		P-value
	Notation	Value			Notation	Value	
Const	β 0	12149.44	< 0.0001	D2	β44	-1590.04	0.0207
A	β1	0.764174	0.744	G2	β77	0.000462	< 0.0001
B	β2	-1.28627	0.001	AJ	β19	-0.00225	0.0124
C	β3	2.198179	0.070	CE	β35	-3.04592	0.0595
D	β4	4936.285	0.256	DG	β 47	-0.35292	0.0285
E	β5	451.0313	0.881	FG	β 67	0.000859	< 0.0001
F	β6	-2.74145	0.0003	FJ	β 69	0.001773	< 0.0001
G	β7	-4.49152	< 0.0001	GH	β 78	0.011388	0.0005
H	β8	-29.4091	0.0088	GJ	β 79	0.001715	< 0.0001
J	β9	-4.76686	< 0.0001	-	-	-	-

Table 5- 4 Simplified Response Surface Model of TH-169 Mainline TTT

Term	Coefficient		P-value	Term	Coefficient		P-value
	Notation	Value			Notation	Value	
Const	β 0	14125.01	< 0.0001	D2	β44	-1616.02	0.0216
A	β1	0.797669	0.6836	G2	β77	0.000559	< 0.0001
B	β2	-1.17835	0.0038	J2	B99	0.004375	< 0.0001
C	β3	2.361605	0.2322	AJ	β19	-0.00233	0.0114
D	β4	5105.397	0.236	CE	β35	-3.15328	0.0567
E	β5	474.5358	0.9695	DG	β 47	-0.39653	0.0163
F	β6	-3.18038	< 0.0001	FG	β 67	0.000965	< 0.0001
G	β7	-5.31521	< 0.0001	FJ	β 69	0.003839	< 0.0001
H	β8	-26.871	0.0396	GH	β 78	0.010503	0.0016
J	β9	-18.2614	< 0.0001	GJ	β 79	0.004109	< 0.0001

Table 5- 5 Simplified Response Surface Model of TH-169 Ramp TTT

Term	Coefficient		P-value	Term	Coefficient		P-value
	Notation	Value			Notation	Value	
Const	β 0	-1160.93	< 0.0001	G2	β77	-9.8E-05	0.0216
A	β1	-0.57639	0.6836	J2	B99	-0.00301	< 0.0001
B	β2	4.845511	0.0038	AE	β 15	0.713006	< 0.0001
C	β3	-1.63918	0.2322	BG	β27	-0.00206	0.0114
E	β5	-1148.06	0.9695	CG	β 37	0.00065	0.0163
F	β6	0.438926	< 0.0001	FG	β 67	-0.00011	< 0.0001
G	β7	0.878759	< 0.0001	FJ	β 69	-0.00207	< 0.0001
J	β9	12.72504	< 0.0001	GJ	β 79	-0.0024	0.0016

Table 5- 6 Simplified Response Surface Model of I-94 System TTT

I-94:

Term	Coefficient		P-value	Term	Coefficient		P-value
	Notation	Value			Notation	Value	
Const	β 0	18066.13	< 0.0001	G2	β77	0.000833	< 0.0001
A	β1	-0.68867	0.0221	AC	β13	0.003283	0.0591
B	β2	17.14337	0.6459	BD	β24	-11.594	0.0641
C	β3	1.56152	0.3646	BG	β 27	-0.00353	0.0903
D	β4	392.96	0.3759	BH	β 27	0.205763	0.1001
E	β5	126.6405	0.0135	CF	β 36	-0.00337	0.0158
F	β6	-1.47371	< 0.0001	FG	β 67	0.000776	< 0.0001
G	β7	-5.36054	< 0.0001	GJ	β 79	-0.001	< 0.0001
H	β8	-4.89829	0.2131	-	-	-	-
J	β9	2.729135	< 0.0001	-	-	-	-

Table 5- 7 Simplified Response Surface Model of I-94 Mainline TTT

Term	Coefficient		P-value	Term	Coefficient		P-value
	Notation	Value			Notation	Value	
Const	β 0	14797.31	< 0.0001	F2	β66	-0.00076	0.0647
A	β1	-0.54804	0.0936	G2	β77	0.001059	< 0.0001
B	β2	12.82609	0.0078	J2	β99	-0.00482	< 0.0001
C	β3	1.481412	0.1161	AC	β13	0.003459	0.0571
D	β4	384.2433	0.2994	BD	β24	-10.9643	0.0937
E	β5	131.1163	0.0144	CF	β 36	-0.0034	0.0197
F	β6	1.417516	< 0.0001	FG	β 67	0.000985	< 0.0001
G	β7	-6.78507	< 0.0001	GJ	β79	0.001568	< 0.0001
H	β8	1.988263	0.0637	-	-	-	-
J	β9	-0.61584	< 0.0001	-	-	-	-

Table 5- 8 Simplified Response Surface Model of I-94 Ramp TTT

Term	Coefficient		P-value	Term	Coefficient		P-value
	Notation	Value			Notation	Value	
Const	β 0	1125.652	< 0.0001	A2	β11	0.000486	0.0235
A	β1	-1.89862	< 0.0001	G2	β77	-0.00023	< 0.0001
B	β2	9.204244	< 0.0001	J2	β99	0.006122	< 0.0001
C	β3	-0.12553	0.0346	AG	β17	0.000104	0.0869
D	β4	146.9317	0.5583	BG	β27	-0.00334	< 0.0001
F	β5	0.408517	< 0.0001	DJ	β49	-0.40337	0.0956
G	β6	1.272524	< 0.0001	FG	β67	-0.00021	< 0.0001
H	β7	-0.72259	0.0432	FJ	β69	-0.00103	< 0.0001
J	β8	4.812901	< 0.0001	GJ	β79	-0.00256	< 0.0001

Diagnostic Checks

Figures 5-11 and 5-12 present all the important plots in Diagnostic checking for TH-169 and I-94 System TTTs. These plots for diagnostic details can be obtained from Design Expert®. Here studentized residuals (raw residual divided by its standard error $\sqrt{MSE(1-h_i)}$, where h_i is the leverage) are used to counteract varying leverages due to the distribution of design points in the parameter space. The most important diagnostic the normal probability plot of the studentized residuals shows highly linear pattern, for both TH-169 and I-94, indicating that the error term is normally distributed and does not require any transformation. Cook's distance plots does not show any influential points and outliers. Residuals vs Predicted plots show no curvature trend in both sites. This ensures that the models are statistically valid and thus the inferences based on the response surface will be valid.

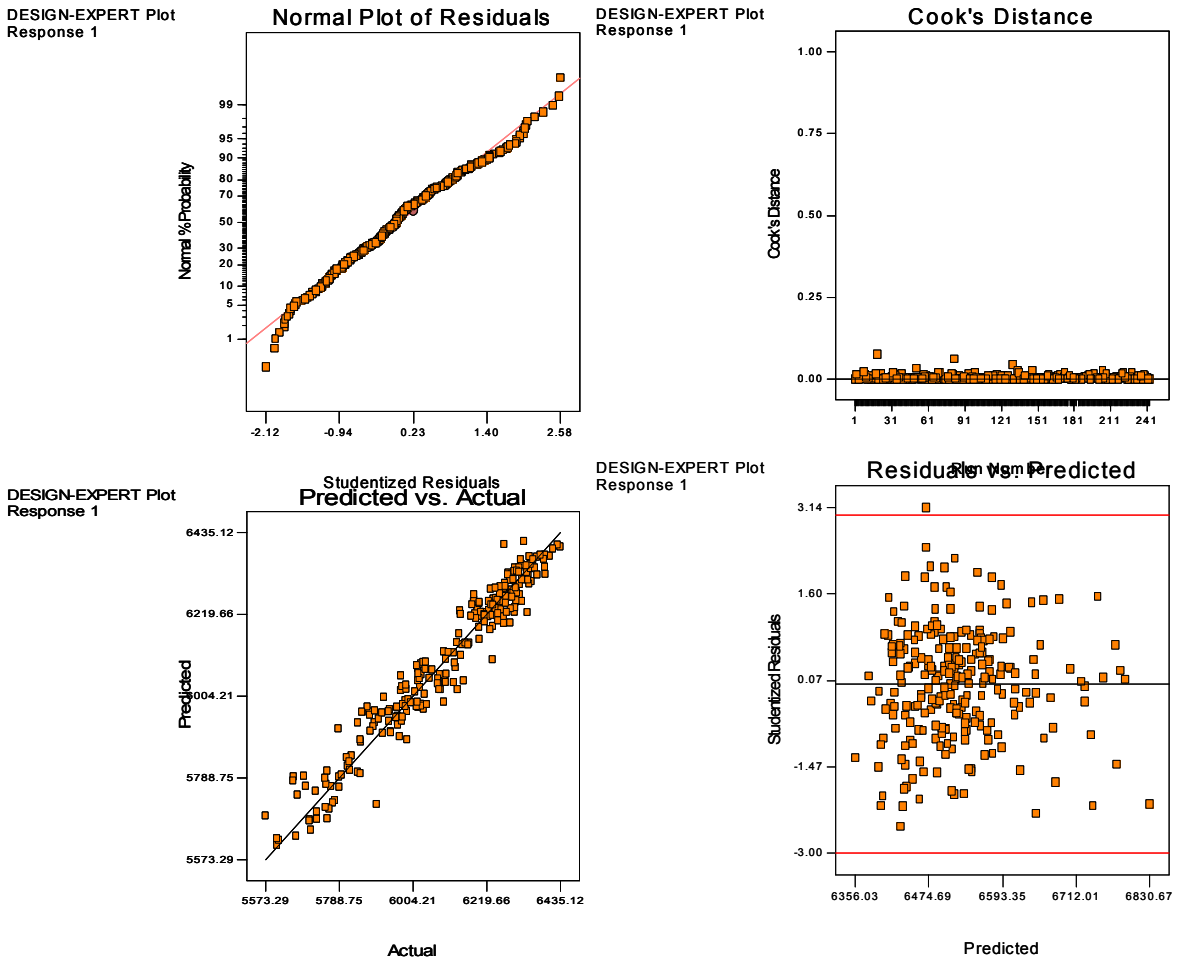

Figure 5- 12 Diagnostics TH-169 System TTT

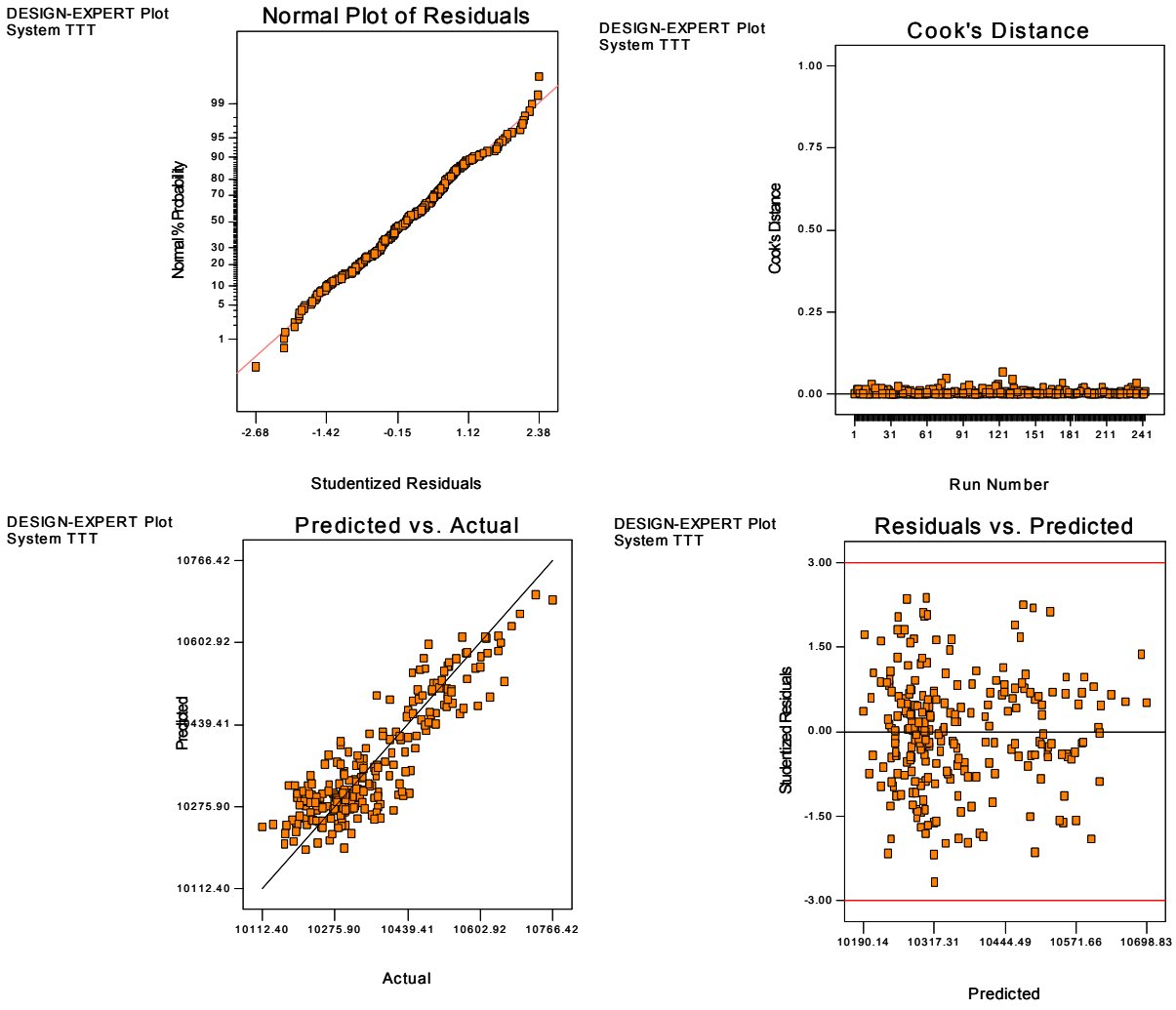

Figure 5- 13 Diagnostics I-94 System TTT

5.4.2. Optimization Results

Scenario 1: (T_{max} free to vary)

The optimization results for scenario 1 are summarized in Table 5.9. The optimal parameter values presented in Table 5.9, suggest that the currently used parameter values are generally different from the optimal values. Moreover, for all the three optimization objectives, optimal parameter values also differ between test sites. This strongly suggests the need for a site specific optimization. TH-169 NB is a moderately congested site while I-94 carries considerable higher volumes of traffic and is heavily congested during the peak period.

Table 5.9 also presents some major MOEs to assess the effect of optimization on the SZM control performance. The base case for all the comparisons was the SZM control operated with the currently used parameter values. On TH-169, System TTT minimization decreased system TTT by 5 percent and Mainline TTT by 8.5%. Further, a considerable decrease of 30% in the number of stops on the mainline was also achieved. Number of stops on the mainline is regarded as a surrogate measure of secondary accidents which are rear end collisions. In this a view, a 30% decrease in number of stops can be regarded as any additional benefit along with overall system and mainline improvement in travel delay. However, these benefits also resulted in TTT increase on all ramps by 40 %. When mainline TTT was minimized, an improvement of 10% in the mainline TTT, 4.5% in system TTT and 34% in number of mainline stops was achieved but with a 73% deterioration in ramp performance. On the other hand, for the severely congested site I-94, system TTT minimization favored ramps to Mainline. System TTT decreased by 3.3 % and Ramp TTT decreased by 44%, while mainline TTT increased by 1.1%. With mainline optimal parameter values, the mainline TTT decreased by 5% over the base case, but ramp TTT increased by 43%. In essence, these results suggest that the optimization is effective in improving the performance of SZM control. However, which specific set of optimal parameter values to use largely depends on the local needs and the level of congestion on the freeway.

Table 5- 9 Optimization Results: Scenario 1*

			TH-169 North Bound			I-94 East Bound		
			Optimization Objective			Optimization Objective		
			STTT	MTTT	RTTT	STTT	MTTT	RTTT
PERFORMANCE MOEs (% Change from Base†)	System TTT		**-5.1 %**	-4.3 %	-1.9 %	**-3.3 %**	-0.4 %	-0.7 %
	Mainline TTT		-8.4 %	**-10 %**	2.3 %	1.1 %	**-5.1 %**	3.4 %
	Ramp TTTT		39.7 %	72.8 %	**-59.5 %**	-44.4 %	43.1 %	**-48.8 %**
	Mainline Speed		5.1 %	6.0 %	-1.5 %	-0.2 %	1.7 %	-2.6 %
	Mainline Total Stops		**-30.2** %	**-34.1 %**	14.3 %	**5.3 %**	**-20.6 %**	15 %
	Mainline Delay/Veh		-22.2 %	-25.6 %	8.9 %	3.6 %	-15.9 %	10.9 %
	Avg. Ramp queue		44.4 %	86.1 %	-80.6 %	-79.5 %	77.5 %	-87.5 %
	Max Ramp queue		37 %	37 %	-36 %	-19.7 %	41.1 %	-31.9 %
	Pollutants	CO	-6.6 %	-6.7 %	-0.6 %	-1.6 %	-2.9 %	0.6 %
		HC	-5.4 %	-4.9 %	-1.3 %	-2.2 %	-2.2 %	0.2 %
		NOx	-7.6 %	-7.6 %	-0.8 %	-2 %	-3.9 %	0.7 %
PARAMETER OPTIMAL VALUES	A (Base†: 1714)		1660	1600	1660	1640	1400	1640
	B (Base : 25)		40	20	40	20	40	40
	C (Base : 150)		180	120	150	150	210	210
	D (Base : 1.15)		1.2	1.2	1.3	1.3	1.25	1.4
	E (Base : 0.8)		0.9	0.7	0.7	0.9	0.7	0.85
	F (Base : 1800)		1800	1800	2100	1900	2050	2050
	G (Base : 2100)		2400	2100	2700	2700	2100	2700
	H (Base : 32)		40	40	30	25	27	30
	I (Base : 240)		420	420	240	300	480	390

A - Absolute Max Release Rate ; B - Occupancy Threshold ; C - Step Increment in ramp demand
D - Meters turn on Threshold ; E - Passage Compensate factor ; F - Right lane Capacity
G - Other lane Capacity ; H - Full Density of a zone ; J - Max. Ramp wait time

***Scenario 1: Max. Ramp Wait Time Threshold free to vary**

†Base Case : Current parameter values of SZM Control

Scenario 2: (T_{max} set to 4 minutes)

The benefits of optimization in scenario 1 require relaxing the Maximum ramp wait time threshold *(T_{max})* from 4 minutes to 7 and 8 minutes for TH-169 and I-94 respectively. As T_{max}, is one of most significant parameters that affect the performance of SZM control and also is most sensitive with respect to drivers , it is of high engineering importance to also address the question "*What if T_{max} is not allowed to change from its base value of 4 minutes, which is politically accepted?"*

As mentioned earlier, the scenario 2 models can be obtained from general scenario 1 models by setting T_{max} to 240 seconds. For scenario 2, optimization results of only TH-

169 are presented and discussed here. Table 5.10 presents the optimal values for the three objective functions. The System TTT optimal values are very effective in improving both system and ramp performances. Compared to the current parameter values, these optimal values decreased the system TTT by 3.5%, ramp TTT by 55% and average ramp queue by 74%. However, marginal effects were observed on the mainline. Similar results were obtained with ramp TTT as optimization objective. However, under mainline TTT optimization also marginal effects were observed. It is worth noting that system and ramp improvements are significant without increasing the Maximum allowed ramp wait time threshold from 4 minutes. Nevertheless for a 10 % decrease in mainline delay and a very significant 35% decrease in number of stops (a surrogate measure of secondary accidents) a new threshold of 7 minutes is necessary. The Space time 3D graphs of mainline density, as presented in Figures 5.14 and 5.15, also support the above important implication.

Table 5- 10 Optimization Results: Scenario 2*

			TH-169 North Bound		
			Optimization Objective		
			STTT	MTTT	RTTT
PERFORMANCE MOEs (% Change from Base†)	System TTT		**-3.5 %**	-2 %	-1.9 %
	Mainline TTT		0.3 %	**-1 %**	2.3 %
	Ramp TTTT		-54.7 %	-16.3 %	**-59.5 %**
	Mainline Speed		-0.4 %	0.6 %	-1.5 %
	Mainline Total Stops		1.8 %	-5 %	14.3 %
	Mainline Delay/Veh		2.2 %	-2.2 %	8.9 %
	Avg. Ramp queue		**-73.9 %**	-27.8 %	-80.6 %
	Max Ramp queue		-11.1 %	0 %	-36 %
	Pollutants	CO	-2.5 %	-6.7 %	-0.6 %
		HC	-2.3 %	-4.9 %	-1.3 %
		NOx	-2.3 %	-7.6 %	-0.8 %
PARAMETER OPTIMAL VALUES	A (Base†: 1714)		1560	1540	1660
	B (Base : 25)		40	40	40
	C (Base : 150)		180	180	150
	D (Base : 1.15)		1.4	1.2	1.3
	E (Base : 0.8)		0.9	0.7	0.7
	F (Base : 1800)		2100	2100	2100
	G (Base : 2100)		2600	2100	2700
	H (Base : 32)		40	38	30
	I (Base : 240)		240	240	240

A - Absolute Max Release Rate ; B - Occupancy Threshold ; C - Step Increment in ramp demand
D - Meters turn on Threshold ; E - Passage Compensate factor ; F - Right lane Capacity
G - Other lane Capacity ; H - Full Density of a zone ; J - Max. Ramp wait time

***Scenario 2: Max. Ramp Wait Time Threshold set to 4 Minutes**

†**Base Case : Current parameter values of SZM Control**

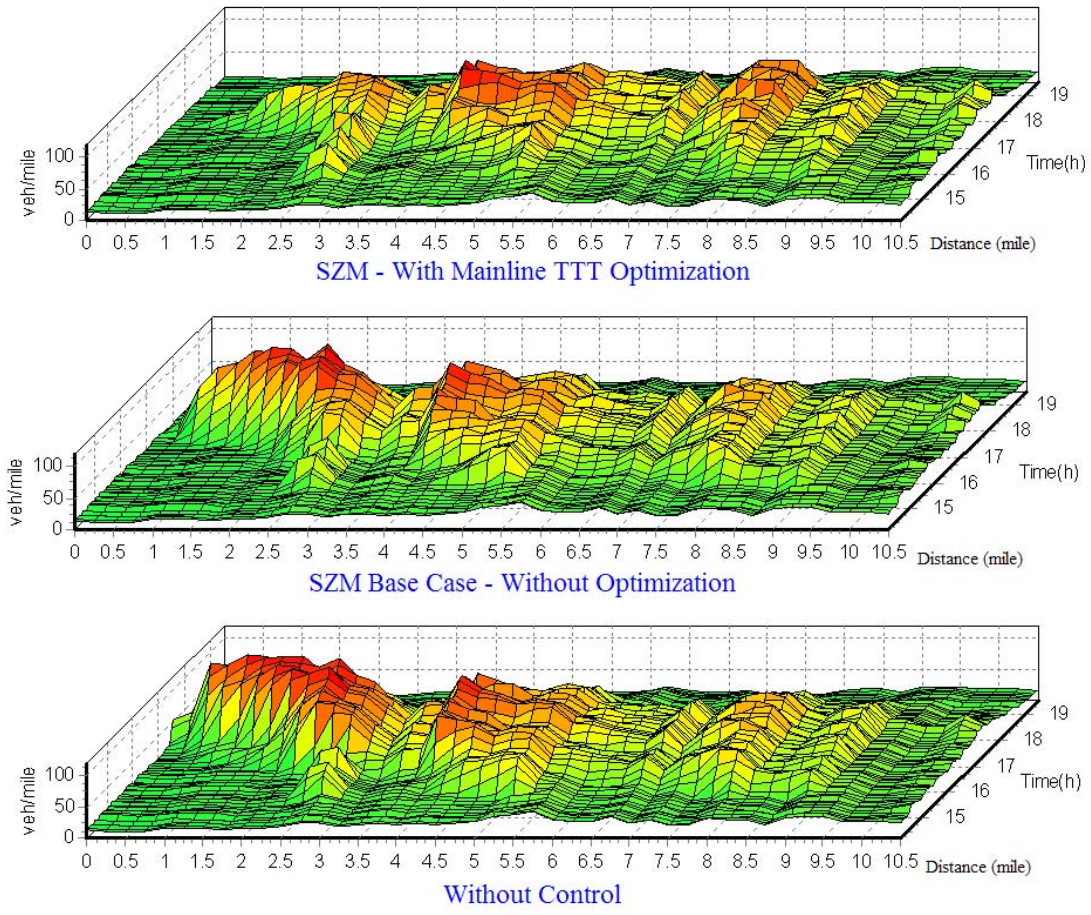

Figure 5- 14 Space-Time 3D plots of TH169 Mainline Density Pattern

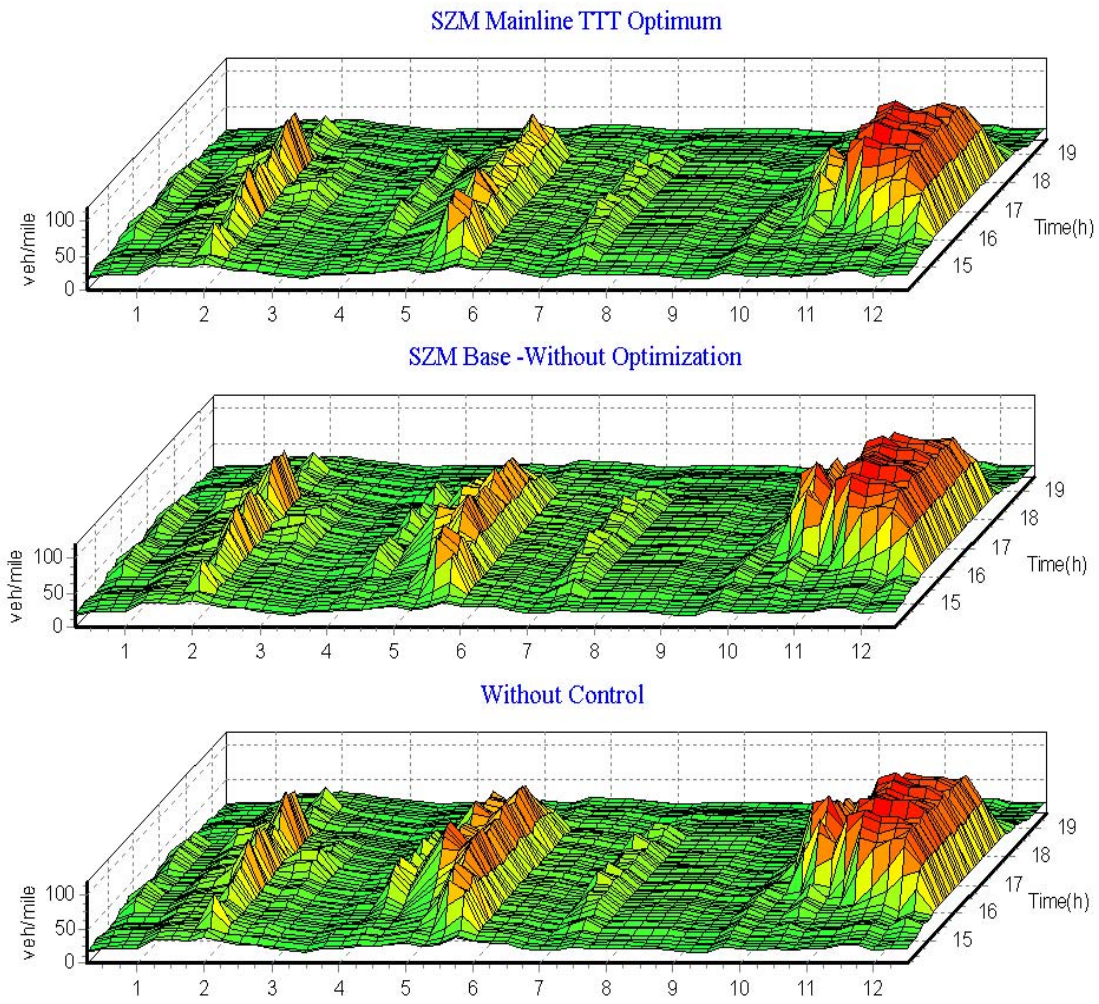

Figure 5- 15 Space-Time 3D plots of I-94 Mainline Density Pattern

Part III Common Parameter Optimization

6. GENERAL METHODOLOGY

The reason why the site-specific optimized parameter values are not suitable for other freeway sections is that different sections have different geometries and traffic patterns. Basically, it is the different congestion levels which lead to inefficiency of the site-specific values. To address it, one intuitive idea is to build a large network for the whole Twin Cities. However, it is infeasible not only because this method is very time-consuming but whether the micro-simulator can handle such a big network is a question. The other easier approach is to build several freeway sections which can represent all the congestion levels. If we can find one set of optimized parameter values which maximally benefits for all these freeway sections simultaneously, we can claim that it is the common optimum parameter set. Therefore, the first step is to identify the representative freeway sections based on the freeway congestion level; the second step is to search the optimum parameter values for all the sections using Response Surface Methodology.

6.1 Representative Freeway Sections

Identifying the representative freeway sections is a crucial step to find the common optimum parameter values. These sections should have geometric properties and traffic characteristics that are representative of the Twin Cities freeway system. In addition, these sections should be able to represent different congestion levels. Based on 2006 metropolitan freeway system congestion report (Mn/DOT, 2007), the Twin Cities' freeway system can be categorized into 4 classes based on 4 congestion levels: Low, Medium, High and Very high. The sections with Low congestion level mean that there is no recurring congestion during peak hour, such as I494 SB, HW100 SB (Figure 1). The sections with Medium congestion level have less than 1 hour of congestion, such as Th36EB, Th169SB. The sections with High congestion level have 1~3 hours of congestion, such as Th169NB. And the sections with Very high congestion level mean that the hours of congestion on these sections are larger than 3 hours. The typical examples are I94EB and I94WB. Combined with the geometric complexity level: Simple, Moderate and Complex, we selected following 4 freeway sections as our research objectives: I-94 EB, TH-169 NB, HW-100 SB and TH-36 EB (Figure 1). And the geometric characteristics are shown in Table 2.

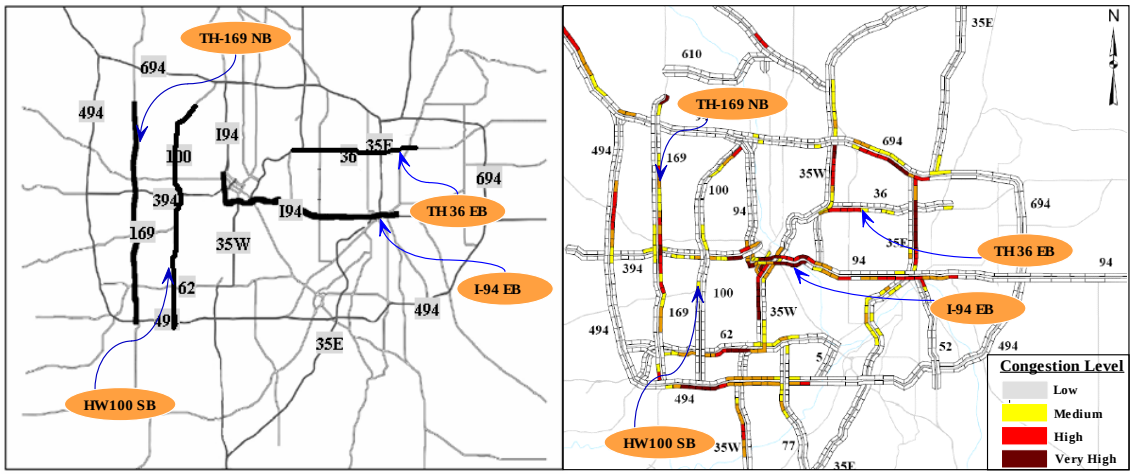

Figure 6- 1 Selected Freeway Sections and Congestion Levels (Mn/DOT, 2007)

Table 6- 1 Characteristics of Selected Freeway Sections

Characteristics	I-94 EB	TH-169 NB	TH-36 EB	HW-100 SB
Direction	Eastbound	Northbound	Eastbound	Southbound
Length (miles)	11	12	7	12
Number of Lanes (Normally)	3~4	2	2	3
Upstream Boundary	I-394 Interchange	I-494 Interchange	I35W Interchange	France Ave
Downstream Boundary	9th St. Off-ramp	63rd Avenue North	TH61 Interchange	I494 Interchange
Metering Period	AM and PM	AM and PM	PM	AM and PM
Metered Entrance Ramps	15	23	8	12
Unmetered Entrance Ramps	4	1	1	10
Off ramps	14	25	9	17
Weaving Sections	6	10	7	15
Lane Drop Locations	3	1	2	3
Geometric Complexity	Complex	Moderate	Simple	Complex
Level of Congestion	Very High	High	Medium	Low

I-94 EB: This test section starts from the interchange with I-394 and ending at 9th St. It is about 11 miles long with 6 weaving sections, 3 lane-drop sections, 19 entrance ramps and 14 exit ramps. The upstream and downstream boundaries are free of congestion. During peak hours, this section is often severely congested due to the heavy traffic and the complex geometry. Therefore, it is the represent of "Very high" congestion level.

TH-169NB: This section is a 12-mile circumferential freeway starting from the I-494 interchange and ending at 63rd Avenue North. The upstream and downstream boundaries are free of congestion. Most of the section has two lanes interrupted by 10 weaving areas, 24 entrance ramps and 25 exit ramps. The 23 metered ramps include 4 HOV bypasses and 2 freeway-to-freeway ramps connecting TH-169 with TH-62 and I-394. It represents the "High" level of congestion because of its high volume and moderate complexity of geometry.

TH-36EB: It is a 7-mile freeway section starting from I35W Interchange to TH61 Interchange with 7 weaving sections, 2 lane-drop sections, 9 entrance ramps and 9 exit ramps. The geometry is very simple because most of the section has only two lanes. But large traffic volume merging from I35W makes the congestion time about 1 hour during PM peak hour, i.e. "Medium" congestion level.

HW-100SB: Originally HW100SB was a 2-lane freeway section but a new lane built in 2006 significantly decreases the congestion level from "Very high" to "Low". A 12-mile section starting from France Ave to I494 Interchange is selected in our study which includes 22 entrance ramps, 17 exit ramps and 15 weaving sections. It has very good traffic condition except little congestion happened between I394 to Th62.

6.2 Optimization Methodology

Response Surface Methodology (RSM) is adopted in our study to optimize the common parameters in SZM strategy not only because of its efficiency but also for the consistency with the previous study (Beegala et al. 2005) which found the site-specific parameter values for SZM control using RSM. Similar as previous study, RSM can draw the response surface which describes the relationship between response(s) and significant parameters which is identified by the sensitivity analysis. So, it is necessary to define the response(s) and significant parameters first.

Response(s)

As a simulation-based optimization problem, many outputs generated by simulator, i.e. MOEs, can be chose as the response(s), such as *System Total Delay*, *Ramp Total Delay*, *System Total Travel Time*, *Average Mainline Speed*, *Total Number of Stops*, etc. In our study, we selected *System Total Travel Time* as the response because our objective is to maximize the total system performance of SZM control.

Significant Parameters

Fully exploring the relationship between all 20 control parameters (Table 1) and response is almost impossible because of numerous combinations between these parameters. For example, assume a 3-level design, for 20 parameters, there are 3^{20}combinations. In other words, we need to run 3^{20} in simulator. Actually, some parameters have no or little impact on response and sensitivity analysis can identify which parameters significantly affect the response. The sensitivity analysis is already done by Beegala et al. (2005). The result is shown in Table 3.

Table 6- 2 SZM Parameters and Levels in Interval of Significance

No.	Parameters for FF Design	Notation	Units	Factor Code	Levels		
					-1	0	1
1	Absolute Maximum Release Rate	$R_{\max}$	Veh/hr	A	1500	1600	1700
2	Occupancy Threshold	O_{lb}	%	B	15	25	35
3	Increment to Ramp Demand	I_{ramp}	Veh/hr	C	120	150	180
4	Passage Compensate Factor	P_c	Veh/hr	D	1.2	1.3	1.4
5	Ramp Meter Turn on Threshold	M_{on}	-	E	0.5	0.7	0.9
6	Capacity Estimate for Rightmost Mainline Lane	C_R	Veh/hr	F	1800	1950	2100
7	Capacity Estimate for Other Mainline Lanes	C_o	Veh/hr	G	2100	2400	2800
8	Full Density of a Zone	D_f	Veh/mile	H	20	30	40
9	Max Allowed Waiting Time on Local Ramps	$T_{\max,L}$	Second	I	240	360	480

RSM Optimization

Response Surface Methodology (RSM) is one of the most suitable and efficient techniques to determine the best combination of parameter values. RSM is a collection of mathematical and statistical techniques for modeling and analysis of complex systems with an objective to optimize its response (Myers and Montgomery, 1995). Basically, RSM fits a surface of the response which describes the relationship between the significant parameters and response using least square regression based on the data points generated by a Factorial Design. The Factorial Design is vital because it determines whether the response surface is accurate or not. Obviously, the full factorial design which evaluates all possible combination of parameter values is generally infeasible because of the numerous computational requirements. For example, it requires 3^9 simulation runs. Therefore, the Fractional Factorial Design (FFD) technique is applied to reduce the number of runs based on the reasonable assumption that the higher order interactions are negligible and only a fraction of full factorial experiment is sufficient to estimate the effects of main parameters and lower order interactions. In our study, it is recommended to use Orthogonal Resolution V Designs because at least a Resolution of five is required to estimate all two factors interactions and an Orthogonal Design is required to ensure

that both the factors and their interactions are uncorrelated (Box and Hunter, 1961; Franklin, 1984 and Suen et al., 1997). To avoid the laborious work, a 3-level Orthogonal Resolution V Design provided by National Bureau of Standards (1957) is adopted in our study. In detail, it needs $3V^{9-4}$=243, which is only a 1/81 fraction of the full factorial design.

After the design is constructed, the new SZM strategy with each parameter combination in the design is simulated on each freeway section and *System Total Travel Time*, i.e. response, is extracted. The response surface equation is generated based on the responses obtained from the simulations of all parameter combinations in the selected design by least square regression method. Because we apply the Orthogonal Resolution V Design which can estimate the all two factors interactions unbiasedly, the second order surface model is built as following:

$$y_G = \beta_{0,G} + \sum_{i=1}^{k} \beta_{i,G} x_i + \sum_{i=1}^{k} \beta_{ii,G} x_i^2 + \sum_{i<j} \sum_{i=1}^{k} \beta_{ij,G} x_i x_j \qquad (6\text{-}1)$$

Where: y_G = *System Total Travel Time* of freeway section G;

$G \in \{\text{I94EB}, \text{TH169NB}, \text{Th36EB}, \text{HW100SB}\}$;

x_i = Parameter i; $i \in \{1,2,3,4,5,6,7,8,9\}$;

$\beta_{0,G}, \beta_{i,G}, \beta_{ii,G}, \beta_{ij,G}$ = Coefficients of surface model of freeway section G;

$k = 9$, number of parameters.

And the total combined surface function for 4 freeway sections is as Formula :

$$Y = \sum_G y_G = \sum_G \beta_{0,G} + \sum_G \sum_{i=1}^{k} \beta_{i,G} x_i + \sum_G \sum_{i=1}^{k} \beta_{ii,G} x_i^2 + \sum_G \sum_{i<j} \sum_{i=1}^{k} \beta_{ij,G} x_i x_j \qquad (6\text{-}2)$$

Where: Y = *System Total Travel Time* for 4 freeway sections.

Numerically minimize Formula (6-1), we can get the site-specific optimum parameter values for each freeway section. And numerically minimize Formula (6-2), we can get the common optimum parameter values.

7. IMPLEMENTATION AND RESULTS

7.1 Simulator

Obviously, field operational tests are infeasible due to the cost, time and safety considerations. In this study, the AIMSUN simulator was used based on earlier experience, suitability, reputation as well as its proven record in testing traffic control and management systems including ramp metering (Hourdakis and Michalopoulos, 2002).

7.2 Test Dates

The test dates for I94EB and TH169NB are November 01 and November 08, 2000 respectively. The dates represent incident free conditions and were specifically selected during the ramp meter shutdown period to ensure the calibrated simulation models have no systematic bias to a particular set of control parameter values. However, the test dates for TH36EB and HW100SB are February 15 and March 22, 2007 respectively because both freeway sections are rebuilt recently and we only can extract the recent loop detector data from Mn/DOT's website to build the traffic demand for simulation. These two days are also incident free. The afternoon peak was selected for four test sites since all sections experience congestion during that time. In order to include the entire congestion cycle each simulation experiment was conducted from 14:00 to 20:00, while the SZM control period lasts from 15:00 to 18:00.

7.3 Results

Follow the optimization method introduced in previous section, the common optimum parameter values and corresponding MOEs for 4 freeway sections are presented in Table 4. For comparison, the site-specific optimum parameter values as well as corresponding MOEs are described in Table 4 too. This table shows the percentage change between the original SZM control and the improved SZM control with common or site-specific optimum parameter values for 4 test sites. The base case for the comparison is the original SZM control. Thus, a positive percentage change means that this MOE increased with the improved SZM strategy in this freeway section and vice versa.

Measures of Effectiveness

As indicated in Table 4, the common optimum parameter values are different with original values and also differ with site-specific optimum parameter values. But consistent with our expectation, with common optimum values, the *System Total Travel Time* is reduced for all test sections and the reduction varies from 2.18% to 4.96% depending on different type of freeway section. For most test sites, the *Mainline Total Travel Time* has a little reduction but the *Ramp Total Travel Time* as well as *Ramp Delay* significantly decreases. The highest *RTTT* saving is 50.58% for TH-169 NB. Even lowest *RTTT* saving is as much as 17.84% for HW-100 SB. And the decrease of the *Average*

Ramp Delay is about 50.47%. The *System Average Speed* is increased varying between 3.01% and 5.27%. In addition, the *Fuel Consumption* and *Pollutants* are also reduced.

As indicated in Table 4, the reduction of *System Total Travel Time* with common optimum parameter values is lower than with site-specific optimum values for all the test sections. But the difference is not very big. For example, at I-94 EB, the *STTT* decreases 2.86% for common optimum values while 3.07% for site-specific optimum values. And for HW-100SB, the difference of *STTT* saving between two sets of optimum values is only 0.31%. Therefore, although the improvement with the common optimum parameter values is not as good as with site-specific, the difference is not very big and is acceptable.

Optimum Parameter Values

It is necessary to check whether the 9 optimum parameter values are reasonable and to see how they work. An interesting phenomenon is that for all 4 freeway sections, the biggest improvements are all achieved from ramps. This can be shown from Table 4 that the *Ramp Total Travel Time* as well as *Ramp Delay* significantly decreases while the *Mainline Total Travel Time* only has a little reduction. It means that we relax the ramp constraint and let more vehicles merge into freeway system. This phenomenon is consistent with the change of the parameters. As can be seen in Table 4, the *Estimated Capacity Value for Rightmost Lane* increases from 1800 veh/hour/lane in original control to 2100 veh/hour/lane in optimum control, and the *Estimated Capacity Value of Other Lanes* increases from 2100 veh/hour/lane to 2611 veh/hour/lane. The big increase of the capacity value attracts more vehicles releasing from ramps and decrease the ramp wait times. Actually, the change of the capacity value also consists with the real world traffic conditions. In one of our ongoing researches about capacity estimation (Liu et al., 2007), we found that current estimated capacity value most of the time underestimates the real capacity. And the optimum result proves this point.

The other big change happens to "Ramp Turn-on Threshold" which varies from 0.8 in original control to 0.5 in optimum control. The smaller number of turn-on threshold means the ramp metering control will work earlier. This change indicates that in most situations, the ramp metering control is more efficient than no control.

Finally, it is worth to point out that the common optimum values still keep the "Max. Ramp Wait Times" unchanged. Therefore, with the common optimum parameter values, the improved SZM control does not violate the ramp waiting time constraint. Actually, the improved SZM control reduces the ramp wait times because the *Ramp Delay/Veh* is significantly decreases.

Table 7- 1 Optimization Results

Category	%			I-94 EB		TH-169 NB		TH-36 EB		HW-100 SB	
				Site-specific	Common	Site-specific	Common	Site-specific	Common	Site-specific	Common
Performance MOEs (% Change from Base*)	System Total Travel Time			-3.07%	-2.86%	-5.55%	-3.21%	-5.75%	-4.96%	-2.49%	-2.18%
	Mainline Total Travel Time			-0.55%	0.94%	-12.96%	-0.16%	-0.14%	-0.37%	-0.38%	-0.16%
	Ramp Total Travel Time			-26.39%	-38.18%	74.00%	-50.58%	-46.72%	-38.50%	-18.80%	-17.84%
	Mainline Speed			0.02%	-0.34%	8.58%	0.02%	0.06%	-0.02%	0.12%	0.08%
	Mainline Total Stops			-4.59%	2.41%	-41.47%	3.43%	-2.56%	-3.51%	-9.98%	-2.44%
	Mainline Delay/Veh.			-1.23%	3.15%	-26.67%	-0.36%	-0.73%	-2.07%	-4.20%	-1.22%
	Ramp Delay/Veh			-44.74%	-64.88%	104.57%	-65.60%	-56.76%	-47.03%	-27.42%	-24.37%
	System Average Speed			2.54%	3.01%	2.77%	5.27%	5.45%	4.43%	4.83%	4.08%
	Fuel Consumption			-0.96%	-0.40%	-10.08%	-1.86%	-1.93%	-1.58%	-1.97%	-1.81%
	Pollutants	CO		-3.74%	-4.25%	-4.77%	-4.25%	-3.17%	-2.84%	-4.77%	-4.25%
		HC		-2.40%	-2.53%	-2.75%	-2.53%	-4.21%	-3.76%	-2.75%	-2.53%
		NOx		-2.72%	-2.95%	-3.20%	-2.95%	-3.49%	-3.13%	-3.20%	-2.95%
Parameter Optimum Values	Absolute Max. Release Rate		1714*	1640	1400	1714	1400	1500	1400	1714	1400
	Occupancy Threshold		25*	40	40	40	40	15	40	15	40
	Increment to Ramp Demand		150*	210	210	210	210	120	210	210	210
	Passage Compensate Factor		1.15*	1.2	1.2	1.2	1.2	1.4	1.2	1.2	1.2
	Ramp Turn-on Threshold		0.8*	0.7	0.5	0.9	0.5	0.9	0.5	0.9	0.5
	Capacity of Rightmost Lane		1800*	2050	2100	2100	2100	2100	2100	1838	2100
	Capacity of Other Lanes		2100*	2550	2611	2100	2611	2800	2611	2800	2611
	Full Density in a Zone		32*	25	20	40	20	20	20	40	20
	Max. Ramp Wait Times		240*	300	240	480	240	480	240	240	240

*Current parameter values of SZM control

Part IV Concluding Remarks

8. CONCLUSIONS

This study aims to explore both site-specific and common optimum parameter values for ramp control strategies. First, this research presented the potential of Response Surface Methodology supplemented by sensitivity analysis, in optimizing the site-specific performance of Minnesota's New Stratified Zone Metering. At the same time, as the optimization process is general, the proposed methodology can be applied to any ramp control strategy with well defined control parameters. The methodology has also proved effective in determining the optimal parameter values under multiple optimization objectives. Optimal parameter values and the improvement vary by site and optimization objective.

However, the site-specific optimum values have certain shortcomings including the difficulties in implementation and numerous time-consumption to search the site-specific optimum values for all the freeway sections. Therefore, the second objective of this study is to explore the common optimum parameter values for improving Minnesota's Stratified Zone Metering (SZM) Strategy for Twin Cities to replace the site-specific optimum values. Four typical freeway sections which can represent all types of freeway sections in Minneapolis-St. Paul metropolitan area are built in a micro-simulator and the MOE (i.e. *System Total Travel Time*, in this study) of different combinations of the control parameter values which are decided by a Fractional Factorial Design (FFD), are extracted from simulation as the response. Then a response surface, which describes the relationship between response and the combinations of control parameter values, is constructed applying Response Surface Methodology (RSM). This surface is described by a second order mathematical model and the optimum values are estimated by numerically solving it. The common optimum parameter values are implemented in SZM control to compare with the original strategy as well as the control with site-specific optimum parameter values by simulation. The testing results show that the control performance is improved. For example, the *System Total Travel Time* is reduced as much as 4.96%; the *System Average Speed* is increased as much as 5.27%. And the *Mainline Total Stops, Ramp Total Travel Time, Ramp Delay, Energy Consumption* and *Pollutant* decreases as much as 3.51%, 50.58%, 65.60%, 1.86% and 4.25% respectively. In addition, compared with the SZM control with site-specific optimum parameters, the testing results indicated that although the improvement of SZM control with common optimum parameter values is not as good as with site-specific optimum values, the average difference is only 0.91% for 4 test sites. Most importantly, the improved SZM with common parameter values does not violate the ramp waiting time constraint.

It is need to know that the optimization is done for original SZM control. With recent improvements of SZM, such as improved queue control logic and real-time capacity estimation (Liu, et al, 2007), it is desired to apply the optimization method to the improved SZM control to achieve the maximum benefits.

References

Barceló, J., Ferrer, J.L., and Grau R. (1994) *AIMSUN2 and the GETRAM simulation environment.* Internal report, Departamento de Estadística e Investigación Operativa. Facultad de Informática. Universitat Politècnica de Catalunya.

Bogenberger, K., and May, A.D. (1999). Advanced Coordinated Traffic Responsive Ramp Metering Strategies. California PATH Paper *UCB-ITS-PWP-99-19*

Box, G.E.P and Behnken, D.W. (1960). "Some new three-level designs for the study of qualitative variables." *Technometrics* 2, 455-475.

Box, G.E.P, and Hunter, J.S. (1961). "The2^{k-p} fractional factorial designs." *Technometrics* 3: 311-351,449-458.

Box, G. E. P., and Wilson, K.B. (1951). On the experimental attainment of optimum conditions. *Journal of Royal Statistical Society, Series B* 13 (1): 1-38.

CAMBRIDGE SYSTEMATICS (2001). *Twin Cities ramp Meter Evaluation*, Final Report, Minnesota Department of Transportation, St. Paul, MN, 2001.

Cook, R. D, and S., Weisberg (1999). *Applied Regressional Analysis Computing and Graphics*. New York: Wiley.

Craney, Trevor A., and Surles, James G. (2002). "Model-dependent variance inflation factor cutoff values." *Quality Engineering*, v 14, n 3, 2002, p 391-403

Critchfield, G.C., and Willard, K.E. (1986). "Probabilistic Analysis of Decision Trees Using Mote Carlo Simulation," *Medical Decision Making*, 6(1):85-92.

Chang, T.H., and Li, Z.Y. (2002). "Optimization of mainline traffic via an adaptive coordinated ramp-metering control model with dynamic OD estimation." *Transportation Research* 10C: 99-120.

Chu, L., and Yang, X. (2003). *Optimization of the ALINEA Ramp-metering Control Using Genetic Algorithm with Micro-simulation*. 82nd Transportation Research Board Annual Meeting, Washington D.C., 2004.

Elefteriadou, L (1997). "Freeway Merging Operations: A Probabilistic Approach." *Proceedings of the 8th International Federation of Automatic Control Symposium on Transportation Systems*, Chania, Greece, pp. 1351-1356.

Federal Highway Administration. (1990) *Highway Statistics*, Washington, DC.

Franklin, M.F. (1984). "Constructing tables of minimum aberration p^{n-m} designs." *Technometrics* 26:225–232.

Fries, A., and Hunter, W.G. (1980). "Minimum aberration 2^{k-p} designs." *Technometrics* 22: 601-608.

Garib, A., A. E. Radwan, and Al-Deek, H. (1997). "Estimating Magnitude and Duration of Incident Delays." *Journal of Transportation Engineering*. Vol. 123, No. 6, November/December 1997. pp. 459-466.

Geldermann, J., and Rentz, O (2001). "Integrated Technique Assessment with Imprecise Information as a Support for the Identification of Best Available Techniques (BAT)," *OR Spektrum*, 23(1):137-157.

Gipps, P.G. (1986). "A model for the structure of lane-changing decisions." *Transportation Research B* 20B(5) 403-414.

Goldberg, D.E. (1989). *Genetic Algorithm in Search. Optimization and Machine Learning*. Addison-Wesley Pub. Co., Inc.

Golob, Thomas F., Wilfred W. Recker, and Leonard, John D. (1987). "An Analysis of the Severity and Incident Duration of Truck-Involved Freeway Accidents." *Accident Analysis & Prevention*. Vol. 19, No. 4, August 1987. pp 375-395.

Hasan, M., Jha, M., and Ben-Akiva, M.E. (2002). "Evaluation of ramp control algorithms using microscopic traffic simulation." *Transportation Research 10C*: 229-256.

Highway Capacity Manual (2000). Transportation Research Board, National Research Council, Washington, D.C.

Hourdakis, J., and Michalopoulos, P.G (2002). "Evaluation of ramp control effectiveness in two Twin Cities freeways." 81st Transportation Research Board Annual Meeting, Washington D.C., 2002.

ITS America. (1995) *National ITS Program Plan*, Washington, DC

Nelder, J.A., and Mead, R. (1965). "A Simplex Method for Function Minimization," *Computer Journal* **7:** 308-323.

Jones, B., Janssen, L., and Mannering, F. (1991). "Analysis of the Frequency and Duration of Freeway Accidents in Seattle. Accident Analysis & Prevention." Vol. 23, No. 4, August 1991. pp 239-255.

Kleijnen, J.P.C. (1993). "Experimental design for sensitivity analysis, optimization, and validation of simulation models." In J. Banks, editor, *Handbook of Simulation.* Wiley, New York, NY.

Lau. D. (2001). *Minnesota Department of Transportation: Stratified Metering Algorithm,* Internal Report, Mn/DOT, St. Paul, MN.

Liu, X., Wu, X., Michalopoulos, P., and Hourdos, J. (2007). "Employment of the Traffic Management Lab for the Evaluation and Improvement of Stratified Metering Algorithm – Phase III", *Final Report*. MnDOT, St. Paul, MN.

McCamley, F., and Rudel, R.K. (1995). "Graphical Sensitivity Analysis for Generalized Stochastic Dominance," *Journal of Agricultural and Resource Economics*, 20(2):403-403.

Montgomery, D.C. (1997). *Design and Analysis of Experiments*. Wiley and Sons Ltd.: New York, NY.

Myers, R.H. and Montgomery, D.C. (1995). *Response Surface Methodology, Process and Product Optimization Using Designed Experiments.* Wiley Series.

Nam, Doohee, and Mannering, Fred (2000). "An Exploratory Hazard-Based Analysis of Highway Incident Duration." *Transportation Research* – A. Vol. 34A, No. 2, 2000. pp 85-102.

National Bureau of Standards (1959). "Fractional Factorial experiment designs for factors at two and three levels." *Applied Mathematics Series 54*. US Government Printing Office, Washington, D.C.

Operation TimeSaver (1996). Intelligent Transportation Infrastructure Benefits: and Experienced. FHWA, US Department of Transportation, Washington D.C.

Papageorgiou, M. (1983). *Application of Automatic Control Concepts to Traffic Flow Modeling and Control*. Springer, New York, NY.

Papageorgiou, M., Hadj-Saem, H., and Midddelham, F (1997). ALINEA local ramp metering: summary of field test results. Transportation Research Board, 6th Annual Meeting, Washington, DC.

Park, K, and Carter, B. (1995). On the effectiveness of genetic search in combinatorial optimization. Proceeding of the 1995 ACN symposium on Applied Computing.

Polus, A., and Pollatschek, M. (2002). "Stochastic Nature of Freeway Capacity and its Estimation," *Canadian Journal of Civil Engineering*, Vol 29: pp. 842-852, 2002.

Pearce, V. (2000). *What have we learned about ITS? Chapter 2: What have we learned about Freeway Incident and Emergency Management and Electronic Toll Collection?* Technical Reports & Papers, US Department of Transportation, Washington D.C.

Sethi, V, Koppelman, F, Flannery, C, Bhandari, N. and Schofer, J. (1994). Duration and Travel Time Impacts of Incidents – *ADVANCE Project Technical Report TRF-ID-202*. Evanston, IL: Northwestern University, November 1994.

Stat-Ease, (2003). *Design-Expert® 6 User's Guide*, Stat-Ease, Inc. 2003

Stephanedes, Y., and Chang, K.K. (1993). "Optimal control of freeway corridors." *ASCE Journal of Transportation Engineering* 119, 504-514.

Suen C, Chen H, Wu C.F.J. (1997). "Some identities on q^{n-m} designs with application to minimum aberration designs." *Ann Statist* 25:1176–1188

Sullivan, E. C. (1997). "New Model for Predicting Incidents and Incident Delay." *Journal of Transportation Engineering*. Vol. 123, July/August 1997. pp 267-275.

Transportation Research Board (1994). Special Report 209: *Highway Capacity Manual*. National Research Council, Washington, D.C.

Xin, W., Michalopoulos, P.G., Hourdakis, J., and Lau, D. (2004). "Minnesota's New Ramp Control Strategy: Design Overview and Preliminary Assessment". 83rd Transportation Research Board Annual Meeting, Washington D.C., 2004.

Wattleworth, J.A. (1967). Peak-period analysis and control of a freeway system. *Highway Research Record* 157

Zhang, M., Kim T., Nie X., Jin W., Chu L., and Recker W (2001). Evaluation of On-ramp Control Algorithms. California PATH Research Report UCB-ITS-PRR-2001-36.

Zhange, H., Ritchie, S., and Recker, W (1996). Some general results on the optimal ramp metering control problem. Transportation Research C 4, 51-69.

Appendix A

Design Matrix table for a 3^{9-4} fractional factorial design with a resolution V

Defining relation of the design is

$I = AB^2C^2DF = AB^2CDE = CD^2E^2F^2$

Design Point	A	B	C	D	E	F	G	H	J	TH169 System TTT	I94 System TTT
1	-1	-1	-1	-1	-1	-1	-1	-1	-1	8734.782	10557.77
2	0	0	1	1	-1	-1	0	0	-1	8678.632	10446.84
3	1	1	0	0	-1	-1	1	1	-1	8623.733	10244.69
4	-1	0	0	0	0	0	0	-1	-1	8551.212	10209.72
5	0	1	-1	-1	0	0	1	0	-1	8565.878	10280.99
6	1	-1	1	1	0	0	-1	1	-1	8719.605	10451.44
7	-1	1	1	1	1	1	1	-1	-1	8450.437	10162.95
8	0	-1	0	0	1	1	-1	0	-1	8527.706	10457.49
9	1	0	-1	-1	1	1	0	1	-1	8456.32	10326.26
10	0	0	0	1	0	1	1	1	1	8335.972	10235.88
11	1	1	-1	0	0	1	-1	-1	1	8361.259	10522.56
12	-1	-1	1	-1	0	1	0	0	1	8434.903	10363.49
13	0	1	1	-1	1	-1	-1	1	1	8562.463	10726.53
14	1	-1	0	1	1	-1	0	-1	1	8462.535	10324.21
15	-1	0	-1	0	1	-1	1	0	1	8533.935	10443
16	0	-1	-1	0	-1	0	0	1	1	8461.314	10262.96
17	1	0	1	-1	-1	0	1	-1	1	8430.859	10249.9
18	-1	1	0	1	-1	0	-1	0	1	8477.051	10643.24
19	1	1	1	0	1	0	0	0	0	8604.619	10319.64
20	-1	-1	0	-1	1	0	1	1	0	8563.231	10377.4
21	0	0	-1	1	1	0	-1	-1	0	8613.615	10497.76
22	1	-1	-1	1	-1	1	1	0	0	8432.144	10242.91
23	-1	0	1	0	-1	1	-1	1	0	8546.591	10281.23
24	0	1	0	-1	-1	1	0	-1	0	8421.091	10244.16
25	1	0	0	-1	0	-1	-1	0	0	8632.78	10573.56
26	-1	1	-1	1	0	-1	0	1	0	8592.701	10261.99
27	0	-1	1	0	0	-1	1	-1	0	8699.428	10289.2
28	1	0	1	0	1	-1	-1	-1	-1	8685.811	10495.58
29	-1	1	0	-1	1	-1	0	0	-1	8667.176	10369.11
30	0	-1	-1	1	1	-1	1	1	-1	8639.728	10136.68
31	1	1	-1	1	-1	0	0	-1	-1	8624.842	10188.75
32	-1	-1	1	0	-1	0	1	0	-1	8599.68	10359.56
33	0	0	0	-1	-1	0	-1	1	-1	8639.998	10424.53
34	1	-1	0	-1	0	1	1	-1	-1	8545.841	10207.21
35	-1	0	-1	1	0	1	-1	0	-1	8580.553	10481.66
36	0	1	1	0	0	1	0	1	-1	8484.507	10240.06
37	-1	1	-1	-1	-1	1	1	1	1	8410.804	10248.4
38	0	-1	1	1	-1	1	-1	-1	1	8328.816	10598.43

39	1	0	0	0	-1	1	0	0	1	8433.957	10372.82
40	-1	-1	0	0	0	-1	-1	1	1	8371.898	10616.02
41	0	0	-1	-1	0	-1	0	-1	1	8534.563	10340.46
42	1	1	1	1	0	-1	1	0	1	8521.304	10209.55
43	-1	0	1	1	1	0	0	1	1	8450.479	10345.31
44	0	1	0	0	1	0	1	-1	1	8532.975	10179.66
45	1	-1	-1	-1	1	0	-1	0	1	8519.753	10532.23
46	0	-1	0	1	0	0	0	0	0	8476.047	10368.37
47	1	0	-1	0	0	0	1	1	0	8522.05	10287.35
48	-1	1	1	-1	0	0	-1	-1	0	8579.87	10624.09
49	0	0	1	-1	1	1	1	0	0	8447.018	10191.32
50	1	1	0	1	1	1	-1	1	0	8548.713	10490.71
51	-1	-1	-1	0	1	1	0	-1	0	8471.378	10419.71
52	0	1	-1	0	-1	-1	-1	0	0	8614.307	10529.35
53	1	-1	1	-1	-1	-1	0	1	0	8590.757	10308.56
54	-1	0	0	1	-1	-1	1	-1	0	8580.691	10296.84
55	0	1	0	1	0	-1	-1	-1	-1	8732.247	10400.28
56	1	-1	-1	0	0	-1	0	0	-1	8681.88	10284.29
57	-1	0	1	-1	0	-1	1	1	-1	8594.42	10373.9
58	0	-1	1	-1	1	0	0	-1	-1	8617.481	10326.21
59	1	0	0	1	1	0	1	0	-1	8693.433	10322.05
60	-1	1	-1	0	1	0	-1	1	-1	8642.713	10495.67
61	0	0	-1	0	-1	1	1	-1	-1	8545.619	10300.35
62	1	1	1	-1	-1	1	-1	0	-1	8557.546	10388.24
63	-1	-1	0	1	-1	1	0	1	-1	8535.151	10358.07
64	1	-1	1	0	1	1	1	1	1	8399.679	10353.14
65	-1	0	0	-1	1	1	-1	-1	1	8479.748	10461.31
66	0	1	-1	1	1	1	0	0	1	8239.156	10296.61
67	1	0	-1	1	-1	-1	-1	1	1	8490.676	10619.39
68	-1	1	1	0	-1	-1	0	-1	1	8554.862	10364.75
69	0	-1	0	-1	-1	-1	1	0	1	8503.841	10260.5
70	1	1	0	-1	0	0	0	1	1	8452.537	10297.36
71	-1	-1	-1	1	0	0	1	-1	1	8261.755	10333.97
72	0	0	1	0	0	0	-1	0	1	8515.581	10532.53
73	-1	0	-1	-1	-1	0	0	0	0	8556.517	10216.63
74	0	1	1	1	-1	0	1	1	0	8513.277	10369.97
75	1	-1	0	0	-1	0	-1	-1	0	8589.964	10526.99
76	-1	1	0	0	0	1	1	0	0	8421.174	10247.16
77	0	-1	-1	-1	0	1	-1	1	0	8520.657	10340
78	1	0	1	1	0	1	0	-1	0	8424.694	10247.62
79	-1	-1	1	1	1	-1	-1	0	0	8643.493	10563.25
80	0	0	0	0	1	-1	0	1	0	8695.032	10367.78
81	1	1	-1	-1	1	-1	1	-1	0	8619.669	10236.83
82	1	1	1	-1	0	-1	0	-1	-1	8806.128	10311.12
83	-1	-1	0	1	0	-1	1	0	-1	8561.902	10208.68
84	0	0	-1	0	0	-1	-1	1	-1	8729.887	10441.46
85	1	-1	-1	0	1	0	1	-1	-1	8540.496	10112.4
86	-1	0	1	-1	1	0	-1	0	-1	8658.488	10465.18

87	0	1	0	1	1	0	0	1	-1	8576.739	10322.81
88	1	0	0	1	-1	1	-1	-1	-1	8517.796	10333.24
89	-1	1	-1	0	-1	1	0	0	-1	8505.361	10289.98
90	0	-1	1	-1	-1	1	1	1	-1	8454.451	10307.91
91	-1	-1	-1	1	1	1	-1	1	1	8410.24	10466.6
92	0	0	1	0	1	1	0	-1	1	8396.674	10284
93	1	1	0	-1	1	1	1	0	1	8341.032	10313.48
94	-1	0	0	-1	-1	-1	0	1	1	8468.159	10408.31
95	0	1	-1	1	-1	-1	1	-1	1	8520.286	10192.56
96	1	-1	1	0	-1	-1	-1	0	1	8502.183	10642.85
97	-1	1	1	0	0	0	1	1	1	8356.999	10275.75
98	0	-1	0	-1	0	0	-1	-1	1	8545.4	10593.14
99	1	0	-1	1	0	0	0	0	1	8464.196	10434.82
100	0	0	0	0	-1	0	1	0	0	8495.582	10289.58
101	1	1	-1	-1	-1	0	-1	1	0	8515.732	10491.9
102	-1	-1	1	1	-1	0	0	-1	0	8496.248	10220.92
103	0	1	1	1	0	1	-1	0	0	8465.511	10289.11
104	1	-1	0	0	0	1	0	1	0	8462.104	10378.33
105	-1	0	-1	-1	0	1	1	-1	0	8397.741	10234.78
106	0	-1	-1	-1	1	-1	0	0	0	8616.62	10224.26
107	1	0	1	1	1	-1	1	1	0	8696.656	10293.33
108	-1	1	0	0	1	-1	-1	-1	0	8668.303	10569.69
109	0	-1	0	0	-1	-1	0	-1	-1	8727.948	10277.09
110	1	0	-1	-1	-1	-1	1	0	-1	8587.388	10182.72
111	-1	1	1	1	-1	-1	-1	1	-1	8636.161	10603.07
112	0	0	1	1	0	0	1	-1	-1	8435.624	10287.62
113	1	1	0	0	0	0	-1	0	-1	8652.937	10471.12
114	-1	-1	-1	-1	0	0	0	1	-1	8578.976	10212.49
115	0	1	-1	-1	1	1	-1	-1	-1	8505.057	10353.54
116	1	-1	1	1	1	1	0	0	-1	8411.993	10333.75
117	-1	0	0	0	1	1	1	1	-1	8420.825	10220.12
118	1	0	1	-1	0	1	-1	1	1	8407.687	10437.89
119	-1	1	0	1	0	1	0	-1	1	8453.277	10311.6
120	0	-1	-1	0	0	1	1	0	1	8391.444	10248.53
121	1	1	-1	0	1	-1	0	1	1	8480.375	10331.95
122	-1	-1	1	-1	1	-1	1	-1	1	8511.565	10292.86
123	0	0	0	1	1	-1	-1	0	1	8576.387	10692.46
124	1	-1	0	1	-1	0	1	1	1	8373.85	10295.87
125	-1	0	-1	0	-1	0	-1	-1	1	8510.659	10487.45
126	0	1	1	-1	-1	0	0	0	1	8474.921	10338.87
127	-1	1	-1	1	1	0	1	0	0	8535.626	10271.37
128	0	-1	1	0	1	0	-1	1	0	8522.58	10505.88
129	1	0	0	-1	1	0	0	-1	0	8529.055	10330.49
130	-1	-1	0	-1	-1	1	-1	0	0	8463.502	10306.3
131	0	0	-1	1	-1	1	0	1	0	8469.776	10271.69
132	1	1	1	0	-1	1	1	-1	0	8490.663	10210.79
133	-1	0	1	0	0	-1	0	0	0	8693.894	10288.07
134	0	1	0	-1	0	-1	1	1	0	8505.831	10274.48

135	1	-1	-1	1	0	-1	-1	-1	0	8808.265	10510.35
136	-1	0	-1	1	1	-1	0	-1	-1	8770.8	10310.34
137	0	1	1	0	1	-1	1	0	-1	8698.293	10372.53
138	1	-1	0	-1	1	-1	-1	1	-1	8741.068	10503.78
139	-1	1	0	-1	-1	0	1	-1	-1	8558.505	10220.03
140	0	-1	-1	1	-1	0	-1	0	-1	8539.671	10489.52
141	1	0	1	0	-1	0	0	1	-1	8582.398	10274.41
142	-1	-1	1	0	0	1	-1	-1	-1	8496.124	10252.99
143	0	0	0	-1	0	1	0	0	-1	8503.248	10364.82
144	1	1	-1	1	0	1	1	1	-1	8541.392	10267
145	0	1	0	0	-1	1	-1	1	1	8457.901	10477.66
146	1	-1	-1	-1	-1	1	0	-1	1	8378.225	10261.99
147	-1	0	1	1	-1	1	1	0	1	8448.523	10225.03
148	0	-1	1	1	0	-1	0	1	1	8555.505	10458.3
149	1	0	0	0	0	-1	1	-1	1	8471.492	10187.9
150	-1	1	-1	-1	0	-1	-1	0	1	8552.51	10766.42
151	0	0	-1	-1	1	0	1	1	1	8398.907	10218.98
152	1	1	1	1	1	0	-1	-1	1	8471.55	10515.58
153	-1	-1	0	0	1	0	0	0	1	8444.597	10403.57
154	1	-1	1	-1	0	0	1	0	0	8501.73	10224.41
155	-1	0	0	1	0	0	-1	1	0	8587.47	10656.54
156	0	1	-1	0	0	0	0	-1	0	8512.607	10429.76
157	1	0	-1	0	1	1	-1	0	0	8419.511	10486.26
158	-1	1	1	-1	1	1	0	1	0	8479.361	10277.15
159	0	-1	0	1	1	1	1	-1	0	8430.048	10293.09
160	1	1	0	1	-1	-1	0	0	0	8593.251	10302.57
161	-1	-1	-1	0	-1	-1	1	1	0	8651.731	10299.77
162	0	0	1	-1	-1	-1	-1	-1	0	8682.21	10449.91
163	0	0	0	-1	1	-1	1	-1	-1	8634.254	10291.81
164	1	1	-1	1	1	-1	-1	0	-1	8740.979	10529.8
165	-1	-1	1	0	1	-1	0	1	-1	8631.194	10341.41
166	0	1	1	0	-1	0	-1	-1	-1	8666.229	10413.5
167	1	-1	0	-1	-1	0	0	0	-1	8557.285	10292.6
168	-1	0	-1	1	-1	0	1	1	-1	8498.608	10333.07
169	0	-1	-1	1	0	1	0	-1	-1	8535.542	10318.3
170	1	0	1	0	0	1	1	0	-1	8471.562	10279.37
171	-1	1	0	-1	0	1	-1	1	-1	8581.346	10433.48
172	1	1	1	1	-1	1	0	1	1	8388.991	10166.86
173	-1	-1	0	0	-1	1	1	-1	1	8392.675	10282.03
174	0	0	-1	-1	-1	1	-1	0	1	8473.54	10540.85
175	1	-1	-1	-1	0	-1	1	1	1	8488.57	10264.87
176	-1	0	1	1	0	-1	-1	-1	1	8563.28	10672.29
177	0	1	0	0	0	-1	0	0	1	8530.477	10327.16
178	1	0	0	0	1	0	-1	1	1	8485.554	10476.14
179	-1	1	-1	-1	1	0	0	-1	1	8431.607	10399.18
180	0	-1	1	1	1	0	1	0	1	8445.411	10398.49
181	-1	-1	-1	0	0	0	-1	0	0	8574.991	10495.32
182	0	0	1	-1	0	0	0	1	0	8538.335	10285.55

183	1	1	0	1	0	0	1	-1	0	8433.872	10297.67
184	-1	0	0	1	1	1	0	0	0	8451.046	10316.89
185	0	1	-1	0	1	1	1	1	0	8297.958	10337.13
186	1	-1	1	-1	1	1	-1	-1	0	8472.525	10501.63
187	-1	1	1	-1	-1	-1	1	0	0	8705.698	10199.02
188	0	-1	0	1	-1	-1	-1	1	0	8688.901	10522.24
189	1	0	-1	0	-1	-1	0	-1	0	8620.715	10342.44
190	-1	1	-1	0	0	-1	1	-1	-1	8612.776	10282.47
191	0	-1	1	-1	0	-1	-1	0	-1	8801.435	10528.47
192	1	0	0	1	0	-1	0	1	-1	8711.02	10191.93
193	-1	-1	0	1	1	0	-1	-1	-1	8633.094	10565.9
194	0	0	-1	0	1	0	0	0	-1	8575.071	10233.76
195	1	1	1	-1	1	0	1	1	-1	8456.049	10339.97
196	-1	0	1	-1	-1	1	0	-1	-1	8521.595	10270.43
197	0	1	0	1	-1	1	1	0	-1	8495.217	10223.77
198	1	-1	-1	0	-1	1	-1	1	-1	8481.898	10172.94
199	0	-1	0	-1	1	1	0	1	1	8438.104	10296.69
200	1	0	-1	1	1	1	1	-1	1	8398.61	10196.65
201	-1	1	1	0	1	1	-1	0	1	8520.664	10529.6
202	0	0	1	0	-1	-1	1	1	1	8453.009	10298.82
203	1	1	0	-1	-1	-1	-1	-1	1	8593.14	10573.52
204	-1	-1	-1	1	-1	-1	0	0	1	8571.932	10383.48
205	0	1	-1	1	0	0	-1	1	1	8520.902	10649.32
206	1	-1	1	0	0	0	0	-1	1	8421.518	10372.7
207	-1	0	0	-1	0	0	1	0	1	8397.007	10301.09
208	1	0	1	1	-1	0	-1	0	0	8556.89	10472.24
209	-1	1	0	0	-1	0	0	1	0	8487.393	10203.14
210	0	-1	-1	-1	-1	0	1	-1	0	8457.931	10407.13
211	1	1	-1	-1	0	1	0	0	0	8502.87	10247.1
212	-1	-1	1	1	0	1	1	1	0	8484.798	10206.11
213	0	0	0	0	0	1	-1	-1	0	8455.69	10288.26
214	1	-1	0	0	1	-1	1	0	0	8486.851	10290.56
215	-1	0	-1	-1	1	-1	-1	1	0	8652.616	10549.12
216	0	1	1	1	1	-1	0	-1	0	8608.99	10340.38
217	1	-1	1	1	-1	-1	1	-1	-1	8704.383	10324.54
218	-1	0	0	0	-1	-1	-1	0	-1	8775.52	10538.42
219	0	1	-1	-1	-1	-1	0	1	-1	8740.604	10232.85
220	1	0	-1	-1	0	0	-1	-1	-1	8698.551	10421.98
221	-1	1	1	1	0	0	0	0	-1	8544.74	10293.82
222	0	-1	0	0	0	0	1	1	-1	8616.63	10197.58
223	1	1	0	0	1	1	0	-1	-1	8488.677	10164.53
224	-1	-1	-1	-1	1	1	1	0	-1	8448.04	10281.56
225	0	0	1	1	1	1	-1	1	-1	8424.593	10441.38
226	-1	0	-1	0	0	1	0	1	1	8351.663	10420.4
227	0	1	1	-1	0	1	1	-1	1	8415.399	10313.74
228	1	-1	0	1	0	1	-1	0	1	8435.616	10370.8
229	-1	1	0	1	1	-1	1	1	1	8459.884	10352.16
230	0	-1	-1	0	1	-1	-1	-1	1	8661.941	10612.92

231	1	0	1	-1	1	-1	0	0	1	8523.264	10383.81
232	-1	-1	1	-1	-1	0	-1	1	1	8529.061	10538.44
233	0	0	0	1	-1	0	0	-1	1	8486.199	10295.87
234	1	1	-1	0	-1	0	1	0	1	8358.418	10226.92
235	0	1	0	-1	1	0	-1	0	0	8577.224	10480
236	1	-1	-1	1	1	0	0	1	0	8502.332	10427.55
237	-1	0	1	0	1	0	1	-1	0	8451.717	10288.62
238	0	-1	1	0	-1	1	0	0	0	8467.611	10300.11
239	1	0	0	-1	-1	1	0	0	0	8473.485	10234.56
240	-1	1	-1	1	-1	1	-1	-1	0	8581.238	10450.05
241	0	0	-1	1	0	-1	1	0	0	8582.655	10248.8
242	1	1	1	0	0	-1	-1	1	0	8699.259	10604.32
243	-1	-1	0	-1	0	-1	0	-1	0	8777.344	10185.79